Closely and Grossly: ESX-1 Mediated Membrane Disruption

Morwan Osman

A dissertation
submitted in partial fulfilment of the
requirements of the degree of

Doctor of Philosophy

University of Washington
2018

Reading Committee:
Lalita Ramakrishnan, Chair
David R. Sherman
Kevin B. Urdahl

Program Authorized to Offer Degree:
Molecular and Cellular Biology

University of Washington

Abstract

Closely and Grossly: ESX-1 Mediated Membrane Disruption

Morwan Osman

Chair of the Supervisory Committee:
Lalita Ramakrishnan
Department of Medicine
Department of Immunology
Department of Microbiology

Mycobacterium tuberculosis, the causative agent of Tuberculosis (TB), is an obligate human pathogen. Its ability to survive and spread is dependent upon its ability to survive within human hosts. The RD1 locus, which contains the Type VII ESX-1 secretion system, mediates this subversion at multiple stages in both *Mycobacterium tuberculosis* and *Mycobacterium marinum*. Mutants in this locus are defective for an array of virulence phenotypes, including intramacrophage growth, phagosomal permeabilization, and granuloma formation. These phenotypes have been proposed to be all dependent upon the membrane permeabilizing activity of the ESX-1 system, with the secreted substrate ESAT-6 acting as a pore forming toxin. Using *Mycobacterium marinum* as a model for Mtb, we found that we could measure ESX-1 mediated membrane disruption *in vitro* using a hemolysis assay. We demonstrate that membrane permeabilization requires ESX-1 secretion, but that this membrane permeabilization is absolutely contact-dependent. Analysis of lysed membranes via TEM shows that the manner in which Mm causes gross disruptions in host membranes, as opposed to the structured pores that are usually observed with pore forming toxins. We find that the pore forming activity previously ascribed to ESAT-6 is solely due to the presence of the hemolytic detergent ASB-14, to the extent that ESAT-6 preparations that are totally digested retain hemolytic activity. While we do confirm that ESAT-6 is capable of lysing liposomes *in*

vitro at acidic pH, we do not find this correlates with phagosomal permeabilization. Instead we find that this activity is pH independent, suggested that ESX-1 mediated membrane disruption is operating through some still unknown mechanism. Concurrently, to improve our understanding of membrane disruption, we screened for small molecule inhibitors using hemolysis as an *in vitro* measurement of ESX-1 activity, and identified the seleno-organic compound Ebselen. Ebselen inhibits mycobacterial membrane disruption by inhibiting secretion of the ESX-1 substrates ESAT-6 and CFP-10. Comparisons of ebselen with an inactive analogue suggest that this inhibition is mediated via its cysteine-modifying activity. We find that Ebselen is capable of inhibiting the ESX-1 mediated virulence phenotypes of intramacrophage growth and phagosomal permeabilization. Mass spectrometry analysis finds that the inhibition of secretion is likely restricted to the ESX-1 locus., indicating that ebselen has a possible future as an antivirulence compound.

Acknowledgements and Dedication

The path I took to complete this work was highly unusual and wouldn't have been possible with the help of an immense number of people. I would like to thank my thesis committee for their support, flexibility, and valuable feedback. There is also an incredibly long list of Ramakrishnan lab members and collaborators who I am grateful to. Specifically, I'd like to thank Paul Edelstein for his scientific mentorship; James Cameron, who supported me during my injury and recovery; and Jonathan Shanahan and Kevin Takaki for their scientific and technical expertise. I'd also like to thank Professor Will Conrad, who in addition to being a great mentor, supported me in my return from leave and ultimately pushed for me to move across continents and oceans to complete my doctoral studies. Finally, I'd like to thank my advisor Lalita Ramakrishnan, for making a bet that I'd succeed when I was still in the midst of recovery. Without her patience, creativity, support, and mentorship I would not have achieved my scientific goals.

This work is dedicated to my family, who've always supported and pushed me in my academic pursuits. In particular, I'd like to mention Haboba Hafsa and Haboba Zubayda, who were not able to see me complete my studies.

Table of Contents

Chapter 1: The role of ESX-1 in Mycobacterium tuberculosis

Tuberculosis (TB) is one of humanity's oldest diseases, with genetic analyses tracing its aetiological agent, *Mycobacterium tuberculosis,* back 70,000 years (Comas et al., 2013). TB followed humans out of Africa and blossomed during the Neolithic expansion, growing to become the leading cause of human mortality between the 17th and 19th centuries (Comas et al., 2013; Holmberg, 1990). While mortality of TB has dropped drastically over the past century, TB burden is greater today than it has been at any time in human history (World Health Organization, 2017). TB is now the world's leading infectious disease, infecting 10 million and killing 1.7 million in 2016 (World Health Organization, 2017). Surprisingly, TB is not a particularly infectious pathogen compared to other airborne diseases such as influenza, measles, or chicken pox. A single person will only infect 3-10 individuals throughout a year(van Leth et al., 2008), and only a small minority of those infected will progress to active disease. However, TB is frequently fatal if left untreated, with approximately 50% of cases resulting in death (Tiemersma et al., 2011).

Treatment of TB requires a complex regimen of 2 months of four antimicrobials (rifampicin, isoniazid, pyrazinamide, and ethambutol) followed by 4 months of rifampicin and isoniazid. This regimen is extremely effective, with ~96% of individuals successfully completing TB treatment in the United States within 2 years (Centers for Disease Control and Prevention (CDC), 2017). However, adherence is challenging in the face of inadequate infrastructure and resource limitations in areas where the bulk of TB burden lies, with even freely provided treatment forcing significant financial and time investment from patients who can ill afford it (Mauch et al., 2013). Unsurprisingly, this leads to nonadherence and relapse, increasing the risk of drug resistance (Law et al., 2017). Drug resistant TB falls into two categories, multi-drug

(MDR), resistant to at least rifampicin and isoniazid, and extensively drug resistant (XDR), which is additionally resistant to at least one fluoroquinolone and any of three second-line injectable aminoglycosides. Both MDR and XDR TB are difficult to treat, requiring patients to undergo an 18-24 month drug regimen, with 48% of patients failing to complete treatment (World Health Organization, 2017). Terrifyingly, XDR mortality rates are quite high, nearing pre-antibiotic era levels (World Health Organization, 2017). The introduction of new and repurposed drugs such as bedaquiline and delamanid has not resolved the issue of drug resistance, as resistance to both drugs in the same patient was observed in 2015 (Bloemberg et al., 2015). Thus, there is a pressing need to both develop additional drugs and better understand how Mtb manages to evade host defense mechanisms.

RD1 and the Discovery of ESX-1

In 1905, Robert Koch was awarded the Nobel Prize in Physiology or Medicine for his role in the discovery of the bacilli *Mycobacterium tuberculosis* (Mtb), the causative agent of tuberculosis. At the same time, two French scientists, Albert Calmette and Camille Guérin, began developing a TB vaccine after observing that individuals previously exposed to TB were protected against later infection (Calmette, 1931). They sought to generate an avirulent strain of the bovine bacilli *Mycobacterium bovis* (Mb) to use as a protective vaccine against TB. Following 230 passages on bile medium, they successfully generated an avirulent Mb strain (Calmette, 1931). This strain was named bacillus Calmette-Guérin (BCG), and became the first, and only, approved TB vaccine. BCG proved to be partially effective in preventing child miliary TB, but has limited efficacy against the most common form of the disease, adult pulmonary TB (Tameris et al., 2013). Attempts to develop an improved vaccine have yet to succeed, but

studying the mechanism of BCG's attenuation has provided significant insight into Mtb's ability to combat host defense mechanisms.

Nearly a century after Albert Calmette and Camille Guérin began their work to develop BCG, the primary cause of its attenuation was determined: loss a genetic locus present in virulent Mtb named 'Region of Difference 1' (RD1) (Behr et al., 1999; Guinn et al., 2004; Lewis et al., 2003; Mahairas et al., 1996; Pym et al., 2002). Deletion of the RD1 locus in Mtb resulted in severely attenuated virulence(Lewis et al., 2003), and complementation of BCG with an extended portion of the Mtb RD1 locus partially restored virulence (Pym et al., 2003). Separately, 6kDa Early Secretory Antigenic Target (ESAT-6) was being characterized as a secreted and potent T-cell antigen (Andersen et al., 1995). Humans and other mammals infected with Mtb showed uniform reactivity against ESAT-6 (Andersen et al., 1995; Elhay et al., 1998; Ravn et al., 1999), with deletion attenuating virulence in guinea pigs (Wards et al., 2000). ESAT-6 is also referred to as EsxA, but to minimize confusion I will be referring to it as ESAT-6 in this document. The locus containing *esxA* was determined to contain a secretory system, which was then named ESAT-6 secretion system (ESX), the first Type VII Secretion System (T7SS) identified (Okkels and Andersen, 2004; Tekaia et al., 1999).

ESAT-6 is co-secreted with the 10-kDa culture filtrate protein (CFP-10). ESAT-6 and CFP-10 are cotranscribed within a single operon and together form a 1:1 heterodimeric complex (Renshaw et al., 2005). Both ESAT-6 and CFP-10 are WXG-100 superfamily proteins, which are so named due to a Trp-X-Gly hairpin motif and their approximate length of 100 amino acids. WXG proteins are typically secreted in sets of two, either as homodimers, heterodimers, or rarely, as a fusion of two WXG-100 genes. T7SS and WXG-100 proteins have also been identified in both the phyla *Firmicutes* and the GC rich *Actinobacteria* (Bottai et al., 2017).

Despite their ubiquity, little is known about these proteins aside from their role as secreted substrates.

ESX Secretion in Mycobacteria

There exist 5 paralogous ESX loci in Mtb and Mtb, named ESX-1 (containing ESAT-6 and CFP-10) though ESX-5 (Figure 1.1), with ESX-4 thought to be the parental locus (Newton-Foot et al., 2016). Substrate secretion has been observed for all systems except ESX-2 and ESX-4. ESX systems typically contain one or two secreted WXG-100 superfamily proteins; a set of **E**SX **c**onserved **c**omponents (Ecc proteins), and a mycosin serine protease (MycP) protein (Bitter et al., 2009). With the exception of ESX-4, all ESX secretion systems in mycobacteria are made up of four core components: EccB, a cell membrane associated protein ($EccB_1$); EccC, a transmembrane ATPase of the FtsK/SpoIIIE family presumed to be the translocon ($EccC_{a1}$ and $EccCb_1$), EccD, a complex-associated 11-transmembrane domain protein, and EccE, a cell membrane associated protein. EccB, EccC, EccD, and EccE form a complex in the inner membrane in a 2:2:2:1 ratio (Houben et al., 2012b). A 13 Å structure of the *Mycobacterium xenopi* ESX-5 obtained by electron microscopy was recently published, demonstrating an oligomeric structure with six-fold symmetry (Beckham et al., 2017). This complex lies primarily on the inner membrane and does not span the periplasmic space, so how ESX substrates are transported through these structures remains a mystery.

ESX-1, in addition to mediating virulence associated phenotypes (which will be reviewed in the next section), has been associated with distributive conjugal DNA transfer in *Mycobacterium smegmatis* (Msm) (Coros et al., 2008). Distributive conjugal DNA transfer is an atypical type of conjugation in which a donor cell transfers DNA to a recipient cell, resulting in progeny containing mosaic genomes. Mating efficiency is dictated by ESX-1 function. ESX-1

mutant donor cells have up to 100-fold increased transfer efficiencies, while ESX-1 mutant recipients appear to be unable to accept any detectable amount of DNA(Gray et al., 2016). ESX-1 works in concert with ESX-4 in Msm, with recipient cells requiring ESX-4 in order for DNA conjugation to occur(Gray et al., 2016). While there is little evidence of horizontal gene transfer in Mtb (Boritsch et al., 2014), there is evidence it played a role in its evolutionary transition to a human pathogen (Veyrier et al., 2009).

ESX-3 plays an essential role in metal ion homeostasis, mediating both iron and zinc acquisition in Mtb (Tufariello et al., 2016). ESX-3 is also essential for Mtb *in vitro* growth, a phenotype that can be rescue with metal ion supplemented media(Tufariello et al., 2016). The ESX-3 substrate EsxH has also been proposed play a role in virulence via direct interaction with a component of the ESCRT machinery (Mehra et al., 2013). This interaction inhibits intramacrophage antigen processing and phagosomal maturation during Mtb infection, attenuating activation of $CD4^+$ T-cells during infection (Portal-Celhay et al., 2016).

ESX-2 and ESX-5 are only found in slow growing mycobacteria (Newton-Foot et al., 2016). While little is known about the function of ESX-2, ESX-5 is essential for *in vitro* growth of *Mycobacterium tuberculosis* and *Mycobacterium marinum*, and secretion defects are associated with attenuated virulence(Ates et al., 2015; Bottai et al., 2012; Di Luca et al., 2012). Compared to its paralogs, ESX-5 secretes a large quantity of proline-glutamate/proline-proline-glutamate (PE/PPE) proteins which have been associated with virulence and antigenicity (Abdallah et al., 2009; Ates et al., 2015). The attenuation associated with ESX-5 defects have been proposed to be due to inhibition of PE/PPE secretion, disruption of capsule integrity, and outer membrane permeability (Ates et al., 2015, 2016). ESX-5 function also required for full

ESX-1 function, with ESX-5 mutants showing defects in the ESX-1 mediated phenotypes of membrane disruption (Ates et al., 2016).

ESX-1's Role in Virulence

ESX-1 is critical for the delicate interplay between host and pathogen that occurs during mycobacterial infection. The initial stage of infection occurs following engulfment by a host macrophage, the preferred niche for mycobacterial replication. Pathogenic mycobacteria, like Mtb and Mm, are then capable of inducing macrophage aggregation resulting in the formation of a granuloma, the hallmark structure of TB (Cambier et al., 2014). Pathogenic mycobacteria then exploit the granuloma to aid in bacterial dissemination and growth. Following infection establishment, they induce macrophage necrosis, resulting in escape from the granuloma and into the extracellular space, where they can expand the infection or become transmitted to another host. The ESX-1 locus plays a role in each stage: ESX-1 mutants are defective in intramacrophage growth(Stanley et al., 2003), evasion of phagosomal trafficking (Levitte et al., 2016; MacGurn and Cox, 2007), granuloma formation(Volkman et al., 2004), and macrophage recruitment (Volkman et al., 2010).

During granuloma formation, presence of ESX-1 induces host Matrix Metallopeptidase 9 (MMP9) in epithelial cells neighboring infected macrophages (Volkman et al., 2010). Secretion of MMP9 promotes chemotaxis of additional macrophages to the site of infection, aiding in growth of the infection (Volkman et al., 2010). Inhibition of MMP9 production during infection inhibits granuloma formation and bacterial growth. While these dynamics were originally observed using the *Mycobacterium marinum* and zebrafish model of infection, they correlate with findings from human TB. MMP9 has been demonstrated to be induced in epithelial cells

surrounding lung granulomas, and has been found to be elevated in the cerebrospinal fluid of TB meningitis patients (Elkington et al., 2007; Price et al., 2001).

Hints to ESX-1's function lie in its role in phagolysosomal trafficking. It mediates both inhibition of phagolysosomal fusion (MacGurn and Cox, 2007) and phagosomal permeabilization (Simeone et al., 2012; van der Wel et al., 2007). Phagosomal permeabilization was demonstrated to be ESX-1 dependent in 2007, when van der Wel and colleagues observed that both Mycobacterium *leprae* and Mycobacterium tuberculosis were capable translocating from the phagosome into the cytosol of infected macrophages. Mutants of Mtb that were defective in ESX-1 secretion, as well as BCG, which lacks the ESX-1 locus, were incapable of cytosolic translocation (van der Wel et al., 2007). While mycobacteria contain active mechanisms for avoiding phagolysosomal fusion (Bach et al., 2008; MacGurn and Cox, 2007), fusion has a relatively small effect on intracellular survival (Levitte et al., 2016). On the other hand, phagosomal permeabilization appears to be critical for virulence (Simeone et al., 2012; van der Wel et al., 2007), and triggering cytosolic signals that aid in evasion of host responses (Cambier et al., 2017; Wassermann et al., 2015; Watson et al., 2012).

ESX-1, ESAT-6, and Membrane Disruption

ESX-1 has been hypothesized to mediate virulence through its membrane disrupting activity, a mechanism critical for virulence for other intracellular pathogens (Ray et al., 2009). Mtb ESX-1 mutants are defective in epithelial (Hsu et al., 2003), pneumocyte (Hsu et al., 2003), and erythrocyte lysis (Gao et al., 2004; King et al., 1993; Smith et al., 2008). Following demonstration that a mutant defective in ESAT-6 secretion was attenuated in lung epithelial cell lysis, it was proposed that the ESX-1 substrate ESAT-6 was a lysin responsible for this membrane disrupting activity(Hsu et al., 2003). Hsu went on to demonstrate that purified,

recombinant ESAT-6 was capable of disrupting an artificial lipid membrane bilayer as measured by changes in conductance. While initial studies of Mtb's hemolytic activity suggested that it was contact dependent (King et al., 1993), the hypothesis that ESAT-6 was a secreted lysin was bolstered when it was demonstrated purified ESAT-6 capable of lysing erythrocytes (Smith et al., 2008), macrophages (Derrick and Morris, 2007; Refai et al., 2015; Smith et al., 2008), and pneumocytes (Kinhikar et al., 2010).

The primacy of ESAT-6 was further supported by observations that its secretion was required for membrane disruption. ESX-1 mutations that affected ESAT-6 secretion inhibited *in vitro* membrane disruption and phagosomal permeabilization (Houben et al., 2012a; Smith et al., 2008; van der Wel et al., 2007). However, the observation that ESX-1 substrate secretion is co-dependent(Champion et al., 2014; Fortune et al., 2005); making assigning a phenotype to the secretion of a single substrate impossible. ESX-1 has been demonstrated to secrete five major substrates: EspA, EspC, EspB, ESAT-6 (EsxA), and CFP-10 (EsxB) (Gröschel et al., 2016). EspA and EspC are encoded by the distal *espACD* operon (Fig. 1.1), located 260 kb upstream of the ESX-1 locus. In Mtb, mutations in *espACD*(Garces et al., 2010), *esxB* (Hsu et al., 2003), or *espB* (McLaughlin et al., 2007) abrogate ESAT-6 secretion, and mutations in *esxA* abrogate CFP-10, EspB, and EspA secretion (Fortune et al., 2005). This interdependency has been rigorously demonstrated in *Mycobacterium marinum* using a quantitative mass spectrometry approach (Champion et al., 2014). Therefore, it is likely that attempts to assign phenotypes to ESAT-6 secretion were at the very least, unintentionally testing the loss of CFP-10 and EspB. Further complicating matters, there were several reports that ESAT-6's lytic activity was only observed at acidic pH (de Jonge et al., 2007; Peng and Sun, 2016).

In my thesis work, I sought to further understand the mechanism of ESX-1 mediated membrane disruption, and resolve the contradictions I have observed in the field. While prior studies suggest that ESAT-6 is a secreted lysin, this is not congruent with the observations that mycobacterial membrane disruption is contact dependent. I aimed to clarify these conflicts by directly addressing the assumptions that underlie the ESAT-6 lysin hypothesis. Simultaneously, I identified a small molecule inhibitor of ESX-1-mediated membrane disruption with antivirulent effects. Together, these two projects help clarify the mechanism of ESX-1 mediated membrane disruption while providing us with a new tool for its study.

Chapter 1 Figures

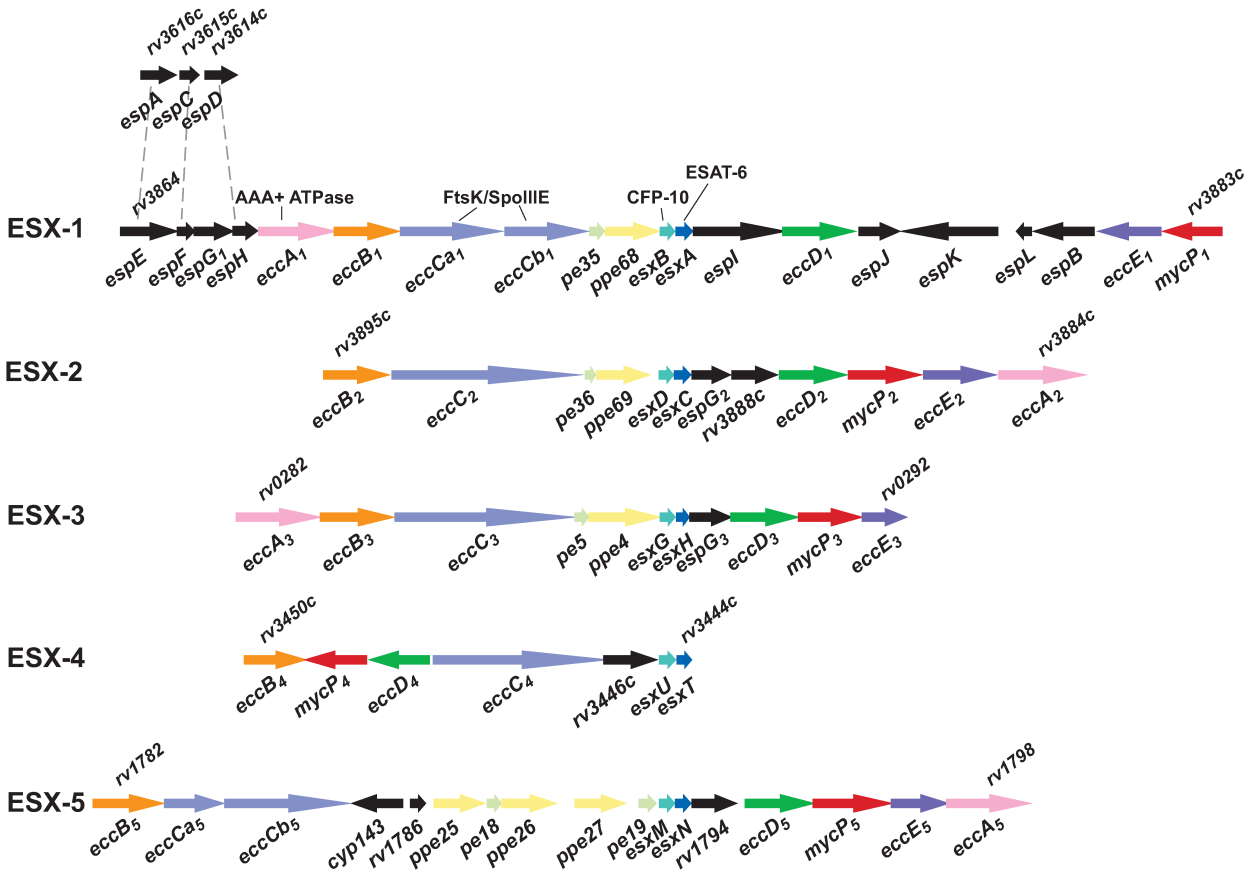

Figure 1.1: Organization of the ESX-1 through ESX-5 genomic loci, along with the *espACD* locus that regulates ESX-1 secretion in Mtb. Components are color coded by family: Pink - EccA, Orange - EccB, Light Blue - EccC, Green – EccD, Yellow – PPE, EsxA – Blue, EsxB – Turquoise, Black – Other/Unknown Function. Figure was adapted from (Bitter et al., 2009) and is licensed under the Creative Commons Attribution license.

Chapter 2: Mycobacterial ESX-1 secretion system mediates host cell lysis through contact-dependent membrane disruption

Summary

Mycobacterium tuberculosis and *Mycobacterium marinum* are thought to exert virulence, in part, through their ability to lyse host cell membranes. The type VII secretion system ESX-1 is required for both virulence and host cell membrane lysis. Both activities are attributed to the pore-forming activity of the ESX-1- secreted substrate ESAT-6 because multiple studies have reported that recombinant ESAT-6 lyses eukaryotic membranes. We too find ESX-1 of *M. tuberculosis* and *M. marinum* lyses host cell membranes. However, we find that recombinant ESAT-6 does not lyse cell membranes. The lytic activity previously attributed to ESAT-6 is due to residual detergent in the preparations. We report here that ESX-1-dependent cell membrane lysis is contact-dependent and accompanied by gross membrane disruptions rather than discrete pores. ESX-1 mediated lysis is also morphologically distinct from the contact-dependent lysis of other bacterial secretion systems. Our findings suggest redirection of research to understand the mechanism of ESX-1-mediated lysis.

Introduction

Tuberculosis is an ancient human disease caused by *M. tuberculosis* that continues to be a leading infectious human killer despite the availability of effective chemotherapeutic regimens(Cambier et al., 2014). There has been a decades-long search to better understand and identify the precise mechanisms by which *M. tuberculosis* causes disease. One virulence determinant that has been identified is a highly immunogenic secreted protein called ESAT-6 (for 6-kDa early secretory antigenic target (Brodin et al., 2004; Gröschel et al., 2016)). ESAT-6 was first identified as a secreted antigen that stimulated T cells (Andersen et al., 1995). Humans and multiple laboratory animal species infected with *Mycobacterium tuberculosis* (Mtb) uniformly show ESAT-6 reactivity (Andersen et al., 1995; Elhay et al., 1998; Ravn et al., 1999). ESAT-6's role in virulence received further support when its deletion in *Mycobacterium bovis* reduced virulence in guinea pigs(Wards et al., 2000).

At the same time as ESAT-6 was being implicated in mycobacterial virulence, parallel work discovered, and ascribed a role in virulence to a specialized secretion system now called ESX-1. Comparisons of the genomes of Mtb and of the attenuated vaccine strain *Mycobacterium bovis* BCG (BCG) revealed a chromosomal region called RD1 (Region of Difference 1) that was missing in BCG (Behr et al., 1999; Mahairas et al., 1996). RD1 was confirmed to play a role in virulence by complementary genetic experiments that showed increased virulence when the region was expressed in BCG, and attenuated virulence when it was removed from Mtb (Lewis et al., 2003; Pym et al., 2002, 2003). *In silico* analysis revealed RD1 to encode ESAT-6 and also part of a previously unidentified secretion system (Mahairas et al., 1996; Tekaia et al., 1999). The presence of this secretion system solved the conundrum of how ESAT-6 is secreted despite lacking a canonical signal sequence (Tekaia et al., 1999). This newly discovered secretion

system was found to contain several other potential secretion substrates, yet it was named ESX-1 (for ESAT-6 Secretion System 1) (Okkels and Andersen, 2004; Tekaia et al., 1999) highlighting the primary role ascribed to ESAT-6 in mycobacterium's pathogenesis (Brodin et al., 2004).

ESAT-6 was first hypothesized to exert virulence by lysing host cell membranes when a transposon insertion mutant in ESAT-6's co-transcribed ESX-1 substrate CFP-10 was found to have lost cytolytic activity for a cultured pneumocyte cell line (Hsu et al., 2003). When purified ESAT-6 and CFP-10 were examined for disruption of artificial lipid bilayers, it was found that that ESAT-6 but not CFP-10 caused membrane lysis (Hsu et al., 2003). These results were confirmed in a series of reports, all implicating eukaryotic cell membrane lytic activity as ESAT-6's virulence mechanism(Derrick and Morris, 2007; Gao et al., 2004; Smith et al., 2008). When transposon mutants in the closely related species, *Mycobacterium marinum* (Mm), were screened to identify those defective for hemolysis, all attenuated mutants were within the ESX-1 locus and were defective for ESAT-6 secretion(Gao et al., 2004). Moreover, the mutants were avirulent and failed to lyse infected macrophages, implicating secreted ESAT-6 in mediating virulence through host cell cytolysis(Gao et al., 2004). Meanwhile, purified recombinant ESAT-6 (rESAT-6) was reported to be capable of disrupting liposome membranes (de Jonge et al., 2007), lysing red blood cells (RBCs)(Smith et al., 2008), and killing cultured macrophages(Derrick and Morris, 2007; Smith et al., 2008). Thus, the experimental evidence from both genetic and biochemical approaches firmly supported the idea that ESAT-6 was responsible for ESX-1-mediated bacterial pathogenicity and was due to its cytolytic activity.

The consensus of contemporary research ascribes a critical role for ESX-1-mediated membranolysis during TB pathogenesis via permeabilization of the mycobacterial phagosome following bacterial entry into host macrophages(Houben et al., 2012a; Simeone et al., 2012; van

der Wel et al., 2007). Phagosomal permeabilization has been found to activate host cytosolic sensing pathways that are exploited by the bacteria for growth and virulence (Dey et al., 2015; Wassermann et al., 2015). By extension, ESAT-6 is held to be directly responsible for phagosomal permeabilization and its downstream pathogenic effects (De Leon et al., 2012; Peng et al., 2016).

In this report, we confirm that a functional ESX-1 secretion system is required for host cell membrane lytic activity and virulence. However, we find that ESAT-6 is not sufficient for ESX-1's lysis of host cell membranes. Rather, we find that the various lytic activities attributed to ESAT-6 at neutral pH are the result of a widely used protocol to isolate ESAT-6, which leaves residual detergent in the preparations. We find that detergent-free ESAT-6 preparations can disrupt liposomes under acidic conditions, as previously observed (De Leon et al., 2012; Ma et al., 2015; Peng et al., 2016). However, this intrinsic low pH-dependent activity of ESAT-6 is not responsible for mycobacterial phagosomal permeabilization in host macrophages.

Results

Mtb ESX-1 Secretion is Linked to Virulence and Hemolysis. We previously showed that deleting the Mm RD1 orthologous region (MTB*AR_5446*-MTB*AR_5455*) results in similar attenuation phenotypes to those reported for Mtb. This strain, Mm-ΔRD1, is attenuated for growth in cultured mammalian macrophages as well as adult and larval zebrafish. The reduced bacterial burdens in the zebrafish are accompanied by increased survival (Swaim et al., 2006; Volkman et al., 2004). To test if the Mm and Mtb ESX-1 systems were functionally equivalent, we complemented Mm-ΔRD1 with a cosmid containing either the Mtb ESX-1 locus (Mm-ΔRD1::*rv3861-rv3885*$_{mt}$, referred to as Mm-ΔRD1::WT$_{mt}$)(Pym et al., 2003) or the Mtb ESX-1 locus bearing a point mutation in the gene encoding ESAT-6 (Mm-ΔRD1::M93T$_{mt}$), which fails to restore virulence in the mouse (Brodin et al., 2005). Similar to the Mtb results, we too found that Mm-ΔRD1::WT$_{mt}$ but not Mm-ΔRD1::M93T$_{mt}$ rescued virulence (Fig. 2.1*A*-*C*). We observed that Mm-ΔRD1::M93T$_{mt}$ had diminished secretion not only of ESAT-6, but also of CFP-10 (Fig. 2.1*D* and *E*), which has been shown to be dependent on ESAT-6 for its secretion in Mtb (Berthet et al., 1998).

ESX-1 function in both Mtb and Mm has been associated with RBC lysis (Gao et al., 2004; Speer et al., 2015). After confirming that wildtype Mm exhibited similar dose-dependent hemolytic activity for sheep, rabbit, horse, and cow RBCs (Fig. 2.S*1*), we used sheep RBCs for subsequent experiments. We found that Mm-ΔRD1 was defective for hemolysis (Fig. 2.1*F*), and furthermore that Mm-ΔRD1::WT$_{mt}$ but not Mm-ΔRD1::M93T$_{mt}$ rescued hemolytic activity (Fig. 2.1*F*). These findings show the functional equivalence of Mtb and Mm ESX-1, and confirm the requirement of ESX-1 secretion for both virulence and cytolytic activity.

ESX-1-Mediated Hemolysis is Contact-Dependent. Prior work had suggested that ESAT-6 mediated ESX-1 membranolytic activity through pore-forming activity (Hsu et al., 2003; Peng et al., 2016; Refai et al., 2015; Smith et al., 2008). If so, mycobacterial culture supernatants should produce hemolysis. However, even concentrated culture supernatants from wild-type (WT) bacteria are not hemolytic (Fig. 2.2*A*). This finding raised the possibility that ESX-1 mediated hemolysis was contact-dependent as was reported by King *et al.* (King et al., 1993). Moreover they showed that only the virulent Mtb strain H37Rv conferred hemolysis; both its avirulent counterpart Mtb H37Ra and *M. bovis* BCG were nonhemolytic. At the time of the King *et al.* publication, it was not known that BCG has the RD1 deletion, which ablates ESX-1 function(Behr et al., 1999; Mahairas et al., 1996), nor that Mtb H37Ra is defective for ESX-1 secretion (Frigui et al., 2008; Mostowy et al., 2004). Reinterpreting the King *et al.* paper in this new light, our finding that mycobacterial supernatants did not confer lysis strongly suggested to us that ESX-1 mediates exclusively contact-dependent hemolysis without any contact-independent lysis. We tested our hypothesis of contact-dependent hemolysis by placing Mm in direct contact with RBCs or by separating bacteria from RBCs using the 0.4 μm cell barrier present in commercially available Transwells. Both WT Mm and Mm-ΔRD1::WT_{mt} were capable of hemolysis only when in direct contact with RBCs (Fig. 2.2*B*). In contrast, *Staphylococcus aureus* retained substantial hemolytic activity when separated by the Transwell barrier consistent with its known ability to secrete hemolytic pore-forming toxins(Vandenesch et al., 2012) (Fig. *2.2B*). These results demonstrated that the hemolytic activity mediated by both Mtb and Mm ESX-1 requires direct bacterial cell contact with host membranes and accounts for essentially all of mycobacterium's hemolytic activity (Fig. *2.2B*).

ESX-1-Dependent Hemolysis is Accompanied by Membrane Disruptions at Points of Bacterial Contact Without Apparent Pore Formation or Host Membrane Penetrating Bacterial Structures. We assessed the morphology of RBC lysis by transmission electron microscopy (TEM). Consistent with our findings in the hemolysis assay, the total number of RBCs was reduced and RBC ghosts were more abundant following incubation with WT Mm, (Fig. 2.3*A*-*C*). Higher magnification views revealed gross RBC membrane disruptions only in WT Mm samples; the few RBC ghosts seen in the Mm-ΔRD1 condition did not have any membrane disruptions (Fig. 2.3*D*-*F*). WT membrane disruptions were predominantly at regions of bacterial contact with RBC membranes (11/12 or 91%) (Fig. 2.3*D*). Mm did not induce discrete pores in the RBCs in contrast to what has been observed for hemolysis caused by classical pore-forming toxins, like *S. aureus* α-hemolysin (Hla)(Freer et al., 1968) and *Clostridium perfringens* necrotic enteritis B-like toxin (NetB)(Fernandes da Costa et al., 2014) (Fig. 2.S2).

The hemolysis assays corroborate the hypothesis that ESX-1 mediates contact-dependent membrane disruption, and show that host cell lysis is accompanied by gross cell membrane disruptions at points of bacterial contact rather than by pore formation. Accordingly, we looked for morphological similarities to contact-dependent cell lysis mediated by specialized bacterial secretion systems of other bacteria. We did not observe any structures mediating contact between Mm and host cells such as the needle structures or pili that have been observed for the Type III Secretion mediated contact-dependent hemolytic activity of *Yersinia enterocolitica* (Hoiczyk and Blobel, 2001) or *Escherichia coli* (Shaw et al., 2001). Moreover, the gross membrane disruptions we observed are in stark contrast to the normal morphology observed for RBCs being lysed upon

contact with Shigella (Clerc et al., 1986). Thus, the mycobacterial ESX-1 secretion system appears to mediate lysis through another distinct mechanism.

Most Membranolytic Activities Attributed to ESAT-6 are due to Residual Detergent in the Preparations. Our findings were contradicted by prior work suggesting that ESAT-6 alone directly lyses membranes by functioning as a secreted pore-forming protein (Hsu et al., 2003; Peng et al., 2016; Refai et al., 2015; Smith et al., 2008). We were puzzled by this discrepancy particularly since we too had previously found that the widely-used, commercially prepared recombinant ESAT-6 (from BEI (Biodefense and Emerging Infections Research Resources Repository)), mediated hemolysis. So too did the rESAT-6 we prepared ourselves using the published protocol (BEI Resources, 2009). Further analysis of the purification protocol revealed that rESAT-6 showed hemolytic activity only when we included the endotoxin removal step – washing of the column with the zwitterionic detergent, ASB-14. When we omitted this wash step, we found the preparation had no hemolytic activity. This result made us wonder if the lytic activity ascribed to ESAT-6 could be due to residual detergent. We compared the hemolytic activity of rESAT-6 prepared side-by-side with and without the detergent wash step, and found that omitting the detergent wash step consistently yielded non-hemolytic rESAT-6 protein preparations (Fig. 2.4*A*). While our experiments were in progress, a paper was published that also found that rESAT-6 only lysed RBCs if the preparations were treated with ASB-14(Refai et al., 2015). These authors interpreted the data to mean that detergent modifies the structure of ESAT-6, activating its lytic activity. If true, the hemolytic activity should be dependent on both ESAT-6 and detergent, and should be abrogated by proteolyzing detergent-treated ESAT-6. However, we found no decrease in hemolytic activity of our rESAT-6 preparations following

Proteinase K treatment (Fig. 2.4*A*). Similarly, Proteinase K treatment also failed to decrease the lytic activity of rESAT-6 obtained from BEI (Fig. 2.4*B*). Yet, Proteinase K treatment completely abrogated the lytic activity of the classic secreted pore-forming toxins Hla and pneumolysin (PLY)(Fig. 2.4*C,D*). In light of these results, we reviewed the ESAT-6 literature and found that publications reporting ESAT-6 cytolytic activity included detergent in the purification as determined from their described methods (Table 2.1). In contrast, those that did not use the detergent step reported ESAT-6 to be devoid of cytolytic activity (Table 2.1). Of note, both we and others (Hsu et al., 2003; Refai et al., 2015) have found that recombinant CFP-10 preparations (including from BEI) fail to lyse cells despite being subjected to the identical detergent wash step as ESAT-6. This suggests that any residual detergent was removed during the subsequent wash and dialysis steps in the case of CFP-10 but not ESAT-6 because of tighter binding of detergent to the latter protein. In summary, we conclude that the cytolytic activity attributed to rESAT-6 is due to residual bound detergent.

ESAT-6 Can Disrupt Liposomes at Acidic pH. While we had ruled out that ESAT-6 functions as a lytic protein at neutral pH, detergent-free rESAT-6 is reported to disrupt liposome membranes at pH ≤5 (Table 2.1, and (De Leon et al., 2012)). We too found that our detergent-free ESAT-6 preparations lysed liposomes at acidic pH <4.5 (Fig. 2.5*A*). Also consistent with the prior report (25), rCFP-10 and an rESAT-6/CFP-10 heterodimer prepared from a bicistronic construct did not lyse liposomes (Fig. 2.5*A*). These findings confirmed that detergent-free ESAT-6 has intrinsic liposome-disrupting activity at acidic pH (De Leon et al., 2012).

ESAT-6's pH-Dependent Membranolytic Activity is not Required for ESX-1-Mediated Macrophage Phagosomal Permeabilization. ESAT-6's lytic activity at acidic pH is thought to

be responsible for ESX-1's ability to permeabilize macrophage phagosomes and allow mycobacteria to access the cytosol (De Leon et al., 2012; Peng et al., 2016). If so, then blocking phagosomal acidification with the vacuolar ATPase (vATPase) inhibitor, Bafilomycin should decrease ESX-1-mediated phagosomal permeabilization. To test this, we first confirmed that Bafilomycin inhibited phagosomal acidification of both WT Mm and Mm-ΔRD1 in the human macrophage cell line THP-1 (Ghigo et al., 2002) by staining with LysoTracker, an acidophilic dye that labels lysosomal compartments (Levitte et al., 2016)(Fig. 2.5*B,C*). Next, we tested the effect of Bafilomycin on mycobacterial phagosomal membrane permeabilization with an assay that uses the FRET based dye, CCF4-AM (Simeone et al., 2012). CCF4-AM is absorbed into the host cytosol and produces a green fluorescent signal (525nm)(Simeone et al., 2012). If the mycobacterial phagosome is permeabilized, then the dye is cleaved by the endogenous Mm cell-surface associated β-lactamase BlaC, which is otherwise inaccessible to the dye. Cleavage causes a loss of FRET and an increase in blue fluorescence (450nm). We observed similar loss of FRET in WT Mm and Mm-ΔRD1, showing they had similar BlaC activity (Fig. 2.S*3*). Thus, phagosomal permeabilization can be measured by the shift from green to blue fluorescence within an infected cell (Simeone et al., 2012). We used this dye to measure the phagosome-permeabilizing ability of WT Mm and MmΔRD1 following treatment with Bafilomycin or vehicle. We confirmed prior findings that permeabilization was increased in WT infection compared to MmΔRD1 (Simeone et al., 2012)(Fig. 2.5*D,E*, Fig. 2.S*4*). However, we found no reduction in permeabilization in Bafilomycin-treated macrophages (Fig. 2.5*E*). Thus, acidification is not a prerequisite for permeabilization of the mycobacterial phagosome, suggesting that ESX-1 mediated phagosomal permeabilization does not occur through the acidic pH-dependent membrane lytic activity of ESAT-6. Rather, it appears that ESX-1 mediated

phagosomal permeabilization proceeds through the same mechanism as RBC lysis that is either independent of ESAT-6 or requires additional mycobacterial determinants.

Discussion

We show that ESAT-6 does not function as a pore-forming protein nor does it possess intrinsic membranolytic activity under physiological conditions. We find, however, that ESX-1 mediates cell lysis occurs through a contact-dependent mechanism that causes gross disruptions at points of bacterial contact. Other specialized bacterial secretion systems are known to mediate contact-dependent cytolysis(Hoiczyk and Blobel, 2001; Shaw et al., 2001). It is tempting to speculate that this might be the case for mycobacteria as well, given a very recent study suggesting that the ESX-1 substrate EspC may form a surface-exposed filamentous structure spanning the mycobacterial cell envelope (Lou et al., 2017). The ESX-1-mediated membrane disruptions we observe in RBCs look similar to the ESX-1-mediated phagosomal membrane degradation of infected myeloid cells as observed by cryoelectron microscopy (Houben et al., 2012a; van der Wel et al., 2007) suggesting that it is relevant to mycobacterial pathogenesis. The intracellular pathogen *Rickettsia* also disrupts phagosomal membranes, and it does so via phospholipase A2 (Walker et al., 2001)in a manner that appears similar to these ESX-1-mediated membrane disruptions. While mycobacterial phospholipases are not involved in Mtb's phagosomal permeabilization (Le Chevalier et al., 2015), some hemolytic activity is attributed to a mycobacterial sphingomyelinase(Speer et al., 2015). In addition, a host phospholipase A2 may be involved in phagosomal permeabilization(Jamwal et al., 2016). Such findings leave open the possibility that ESX-1 regulates the activities of bacterial and host lipolytic enzymes to disrupt membranes. Alternatively, ESX-1-mediated lysis may occur through a secreted component (including ESAT-6) that needs to be activated by a mycobacterial (or even host) membrane component. Such a scenario would make lysis through a secreted lysin contact-dependent, and is exemplified in the case of *Serratia marcescens* hemolysin ShlA . ShlA is secreted and activated

by its partner ShlB only in the presence of phosphateidylethanolamine, a lipid commonly found in biological membranes (Hertle et al., 1997).

Our experiments raise the question of what precise role ESAT-6 plays in mycobacterial virulence. Prior reports that ESAT-6 mutants are defective for host cell lysis (Brodin et al., 2006; Gao et al., 2004; Hsu et al., 2003) are confounded by the finding that several ESX-1 substrates are mutually co-dependent for secretion(Champion et al., 2014; Fortune et al., 2005). However, because it is an immunodominant antigen, it is likely to have a role in virulence. Perhaps it acts downstream of ESX-1 mediated membrane permeabilization to directly influence pathogenesis by regulating immune determinants (Brilha et al., 2017; Chatterjee et al., 2011; Volkman et al., 2010). The finding that ESAT-6 binds to liposomal membranes may reflect its ability to bind lipids and thereby eukaryotic cell membranes (de Jonge et al., 2007; Renshaw et al., 2005) so as to initiate or subvert the requisite cell signalling events. In such a scenario, ESX-1 mediated phagosomal permeabilization would enable ESAT-6 to gain contact with the cytosol of the infected macrophage or even neighboring cells to influence their immune program.

Our quest to confirm and expand the model of ESAT-6 as a cytolytic, pore-forming toxin took an unexpected turn when a serendipitous omission in a well-defined and widely used purification protocol led us to re-examine the biological function that had been widely attributed to this mycobacterial virulence determinant. Our experiments lead us to re-interpret ESX-1's membrane lytic activity. We hope our findings will lead to a better understanding of this and of ESAT-6's biological function.

Acknowledgements. We thank Stanley Falkow for critical review of the manuscript, and David Sherman and Mark Troll for advice and discussion. This work was supported in part by a

Wellcome Trust Principal Research Fellowship, the NIH (grant R37AI054503), and the National Institute of Health Research Cambridge Biomedical Research Centre to L.R.; a National Science Foundation Graduate Research Fellowship Grant DGE-1256082 to M.M.O.; an NIH training grant (T32 AI55396) award to F.C. and Agence National de Recherche grants (ANR‐14‐JAMR‐001‐02 and ANR-10-LABX-62-IBEID) to R.B.

Experimental Procedures

Bacterial Strains. All strains were derived from wild-type Mtb purchased from American Type Culture Collection (strain M, ATCC #BAA-535). RD1-deleted Mm (ΔRD1) was generated as described previously (Volkman et al., 2004).

Zebrafish & Macrophage Experiments. Zebrafish husbandry and experiments were in compliance with guidelines from the UK Home Office and the U.S. National Institutes of Health and approved by the University of Washington Institutional Animal Care and Use Committee. Macrophage infections were conducted in J774A.1 and THP-1 macrophage lines (ATCC).

Production of Recombinant ESAT-6, CFP10, and Pore Forming Toxins

Recombinant ESAT-6, CFP10, and ESAT-6 / CFP10 heterodimer were prepared according to the protocol published by Biodefense and Emerging Infections (BEI) Research Resources Repository (BEI Resources, 2009). *E. coli* strain BL21 was transformed with plasmid pMRLB.7, plasmid pMRLB.46 (obtained through BEI Resources, NIAID, NIH), or plasmid pET29-EsxB-EsxA-6xHis. 10 mL starter cultures were grown to stationary phase overnight and shaking in Luria Bertani broth (Beckton Dickenson #244610) with 100 μg/mL ampicillin (Sigma A0166-5G). These were used to inoculate 1 L of LB media to grow in shaking Fernbach flasks at 37°C. Once cultures reached an OD_{600} between 0.5-0.8, recombinant protein production was induced using 250 μM IPTG (Sigma I5502-1G). Cultures were grown overnight, shaking at 20°C. Bacteria were then pelleted at 4680 x *g* for 30 minutes and resuspended in 10 mL lysis buffer containing 20 mM Tris HCl (pH 7.9), 500 mM NaCl, and 5 mM imidazole. 1 mM

phenylmethylsulfonyl flouride (PMSF, Sigma, P7626-1G) was added as a protease inhibitor immediately prior to lysis. Bacteria were sonicated on ice using an VC505 sonicator (Vibra Cell) with 4x30 s pulses at 30% power. Crude lysates were clarified by centrifugation at 38724 x *g* for 30 minutes at 4°C. For rESAT-6 and rCFP10 1 mL Ni-NTA (Qiagen #30210) columns were equilibrated using lysis buffer. Columns were then washed with 20 column volumes (CVs) of lysis buffer. Next, columns were washed with 10 CVs of 10 mM Tris-HCl (pH 7.9). To one column of rESAT-6, 10 CV of 0.5% ASB14 (Sigma A1346-1G) in 10 mM Tris-HCl (pH 7.9); the other received 10 CV of 10 mM Tris-HCl (pH 7.9). Following detergent or control wash, another 10 CV of 10 mM Tris-HCl (pH 7.9) was added. Recombinant protein was subsequently eluted using 1 M imidazole in 10 mM Tris HCl (pH 7.6). Recombinant ESAT-6/CFP10 heterodimer was purified using a HisTrap HP column (GE Healthcare) equilibrated with Buffer A (20 mM Tris HCl, 150 mM NaCl (pH 7.9) and then eluted with a linear imidazole gradient from 0 mM TO 500 mM in buffer A. Fractions containing heterodimer as observed by SDS-PAGE were then pooled and loaded onto a S200 size exclusion column equilibrated with buffer A (GE Healthcare). Protein-containing fractions, as assessed by A280, were collected for dialysis. Recombinant proteins were subsequently dialyzed in two 4 L stages using 3500 MWCO dialysis tubing in 10 mM Ammonium Bicarbonate (Sigma). Fractions were collected and monitored for recombinant protein elution and purity by SDS-PAGE followed by Coomassie staining. Protein concentration from highly purified eluted fractions were quantified by A280 using a nanodrop 2000 spectrophotometer. Samples were aliquoted and frozen for subsequent use.

Recombinant *S. aureus* α-hemolysin (Hla) and *S. pneumoniae* pneumolysin (PLY) were purified according to methods graciously provided by Julie Bubeck Wardenburg (Personal Communication). Briefly, plasmids #8 and #9 were used to transform BL21 *E. coli*. Isolated colonies were used to inoculate 100 mL LB broth under antibiotic selection and grown overnight at 37°C shaking 120 rpm. 50 mL of culture were used to inoculate 1 L of LB containing selective antibiotic. Samples were then grown on a 37°C shaking incubator until cultures reached OD_{600} = 0.5-0.7. Toxin expression was induced by adding IPTG to a final concentration of 1 mM, and induction was allowed to proceed for 6 hours. Bacteria were then pelleted at 4680 x *g* for 30 minutes. Bacterial cultures were resuspended in 20 mL TGN buffer (50 mM Tris, 150 mM NaCl, 10% glycerol, pH 7.5) containing 1 mM PMSF. Samples were then lysed by French pressure cell. Cell supernatants were clarified by centrifugation at 38724 x *g* for 30 minutes at 4°C. 2 mL Ni-NTA columns were equilibrated in 10 CVs of TGN buffer containing 10 mM imidazole. Samples were then loaded onto Ni-NTA columns by gravity. Samples were then washed with 10 CVs of TGN containing 20 mM imidazole and 50 mM imidazole. Toxin was then eluted using 5 mL TGN containing 250 mM imidazole. Samples were then dialyzed into PBS containing 10% glycerol. Fractions were collected and monitored for recombinant protein elution and purity by SDS-PAGE followed by Coomassie Blue stain. Protein concentration from highly purified eluted fractions were quantified by A280 using a nanodrop 2000 spectrophotometer. Samples were aliquoted and frozen for subsequent use.

Hemolysis & Liposome Lysis Assays. Hemolysis was performed as described previously (King et al., 1993; Smith et al., 2008). Defibrinated sheep red blood cells (sRBCs; Fisher Scientific, Leicestershire, UK) were diluted to a concentration of 1% (v/v) and washed twice with PBS (125

mM NaCl, 16.6 mM Na_2HPO_4, 8.4 mM NaH_2PO_4, pH 7.4) and centrifuged at 3200 x *g* for 5 minutes. Mycobacteria were cultured in 7H9 complete media (middlebrook 7H9 media (Becton Dickenson, # 271310) containing, 0.05% tween 80, 0.2% w/v glycerol, 5 mg/mL bovine serum albumin (BSA, fraction V, Sigma #A3912) 0.005% oleic acid in 0.02N NaOH, 2 mg/mL dextrose, 0.85 mg/mL NaCl) in a humidified CO_2 incubator set to 33 °C and 5% CO2. For hemolysis assays, mycobacteria were inoculated at an OD_{600} = 0.01 from refrigerator stocks and grown until late-log phase (OD_{600} >1). 5 mL of cultures were centrifuged at 3200 x *g* for 10 minutes, and subsequently washed twice with PBS. Assuming 1 OD_{600} unit of bacteria = $3x10^8$ CFU/mL (Peñuelas-Urquides et al., 2013; Veneman et al., 2014), mycobacteria were concentrated to $9x10^8$ mycobacteria in 100 µl. The mycobacteria were then mixed with 100 µl 1% sRBCs in a 1.5 mL microcentrifuge tube and centrifuged at 3200 x *g* for 5 minutes. Samples were incubated for 2 hours at 33 °C. Following incubation, samples were resuspended and repelleted at 3200 x *g* for 5 minutes. 100 µl supernatant was collected and A405 and A540 were measured on a BMG CLARIOstar 96-well microplate reader. Hemolytic activity of PBS was used as a negative control, and hemolytic activity of 0.1% Triton X-100 (Sigma, St. Louis MO) was used as a positive control. Absorbance measurements were converted to percent hemolysis by the following formula:

$$\%\ Hemolysis = \frac{A405\ sample - A405\ negative\ control}{A405\ positive\ control - A405\ negative\ control}$$

To measure hemolytic activity, recombinant proteins were serially diluted in 100 µl PBS and mixed with 100 µl 1% sRBCs in a round-bottom 96-well plate. Recombinant proteins were

prepared as described above. Additional rESAT-6 was obtained through BEI Resources, NIAID, NIH: ESAT-6 Recombinant Protein Reference Standard, NR-14868. Following a 30 minute incubation at room temperature, samples were pelleted by centrifugation at 3200 x *g* for 10 minutes. 100 µl supernatant was transferred to a flat-bottom 96-well plate and hemolytic activity was compared to hemolytic activity of PBS and 0.1% Triton X100 as described above.

To measure hemolytic activity of culture filtrates, 10 µl of culture filtrates were added to 90 µl PBS and 100 µl 1% sRBCs and incubated for 2 hours at 33 °C. Samples were then pelleted and supernatant was collected and assessed for hemoglobin as above.

To measure contact-dependent hemolysis, 100 µl of 1% sheep red blood cells were added to the bottom chamber of a Corning HTS Transwell with 0.4 µm membrane (Sigma #CLS3391) or to a round bottom 96-well cluster plate. 100 µl containing $9x10^8$ CFU of PBS-washed WT Mm, Mm–ΔRD1, or *S. aureus* was added either to the upper chamber of the Transwell or to the round-bottom plate. The 96-well plate was centrifuged at 3220 x g for 5 minutes, and both trays were incubated at 33°C with 5% CO_2. Contact lysis proceeded for 2 hours, while Transwell lysis was allowed to proceed for 24 hours. Following incubation, samples in the lower chamber of the Transwell were transferred to the 96-well cluster plate. All samples were resuspended and pelleted again. Supernatants were collected and assayed for hemolysis as before.

rESAT6, Hla, and PLY were added to RBCs at a final concentration of 0.2, 0.3, and 0.075 mg/ml respectively and incubated at 37°C for 30 min. To assess lytic activity of recombinant proteins

on liposomes, rESAT6, rCFP10, and rESAT6/CFP10 heterodimer were added to liposomes in phosphate-citrate buffer of the indicated pH.

Measuring Liposome Lysis

Liposomes were prepared as previously described (van Rooijen and Hendrikx, 2010). Briefly, cholesterol (Sigma) was dissolved in 99.8% ethanol (Sigma) to 10 mg/mL. Phosphatidylcholine (Egg Yolk Phosphatidylcholine, Sigma) was dissolved in 99.8% ethanol (Sigma) to 100 mg/mL. 86 µl phosphatidylcholine solution was mixed with 80 µl cholesterol solution and ethanol evaporated using N_2 gas and under vacuum. Lipids were resuspended in 400 µl 125 mM ANTS (Biotium) in PBS, gently vortexed and then sonicated in a water bath (55 khz) for 3 minutes. Suspensions were incubated at 4ºC overnight and then washed in PBS by centrifuging at 24000 x *g* for 30 min at 10ºC. Liposomes were then resuspended in 400 µl PBS (~$1.5x10^9$/mL) for use in assays.

For pH buffers 4.0 – 5.0, varied ratios of sodium phosphate and citric acid were combined in 150 mM NaCl. The resulting buffers were verified to have the correct pH, and then diluted 20-fold in 150 mM NaCl to achieve final buffer concentrations. pH was validated again, before and after each experiment.

To measure liposome lytic activity of recombinant proteins, 3 µM rESAT-6, rCFP-10, heterodimer, or equivalent volume of vehicle were added to 100 µl pH buffer. For each condition, 5 µl liposomes were washed twice with the indicated pH buffer and resuspended in 100 µl buffer. Protein and liposome samples were combined in a microcentrifuge tube, and

incubated with shaking at 20°C for 20 minutes. Intact liposomes were pelleted by centrifugation;supernatants were measured for ANTS fluorescence (Excitation⁄Emission (nm): 350±15⁄520±15). Raw fluorescence data was converted to percent lysis using the formula above with buffer as a negative control and buffer containing 0.1% Triton X-100 as a positive control for each pH.

Zebrafish Survival Assays

Adult zebrafish survival following mycobacterial infection was assayed according to Swaim et al. (Swaim et al., 2006). Adult zebrafish were reared in a recirculating aquarium (Aquatic Habitats, Apopka, FL). Weeks prior to infection, adult zebrafish were then moved to a biosafety level 2 flow-through aquarium (Aquatic Habitats, Apopka, FL), and allowed to acclimate. For infection, adult AB zebrafish were anesthetized in a bath of tank water containing 0.1% 3-aminobenzoic acid methyl ester (tricaine). Zebrafish were then infected by intraperitoneal injection of a 10 µl PBS solution containing 100 CFU *Mycobacterium marinum*, diluted from previously quantified and frozen single cell suspensions. 12 fish per condition were infected. One tank was kept per condition. Survival was recorded daily. Tanks were maintained under conditions compliant with laboratory standards outlined by the Institutional Animal Care and Use Committee (water temperature of ~28°C, pH of ~7.4, and conductivity of ~1,500 µS).

Intramacrophage Growth Assays

J774A.1 macrophages (ATCC) were maintained in DMEM (Gibco) supplemented with 10% heat inactivated fetal bovine serum (Labtech), 1% penicillin-streptomycin (Gibco) and 2 mM L-glutamine (Gibco). 24 hours before infection $4.8x10^4$ cells were plated per well in a flat

bottomed 96-well plate. J774A.1 were infected with 0.5-0.75 MOI of tdTomato-fluorescent WT, ΔRD1, ΔRD1::WT and ΔRD1::M93T strain of Mm in antibiotic free DMEM. Media was replaced every 48 hours and course of infection recorded by imaging regularly using an inverted fluorescence microscope for a total magnificationof 100x (Nikon, Eclipse Ti-E). Fluorescence quantification of bacterial burden was assessed as previously described (Takaki et al., 2013).

Measuring Phagosomal Permeabilization

Phagosomal permeabilization was assessed as previously described (Keller et al., 2013). To measure *in vitro* lactamase activity of mycobacteria, $1x10^6$ washed mycobacteria were added to 100 nM CCF4-AM (Invitrogen), 50 ug/mL porcine esterase liver extracts (Sigma) in 100 uL of PBS. This mix was incubated in the dark for 1 hr at 37°C, and a 405nm emission scan was read on a BMG CLARIOstar 96-well microplate reader. THP-1 macrophages (ATCC) were maintained in RPMI-1640 (Sigma) supplemented with 10% heat inactivated fetal bovine serum (Labtech), 1% penicillin-streptomycin and 2 mM L-glutamine. 72 hours prior to infection, cells were stimulated with 33 nM phorbol 12-myristate 13-acetate (Sigma) and plated at $6x10^5$ cells/mL. Activated THP-1s were infected with single-cell suspensions of tdTomato labelled WT and Mm–ΔRD1 (66) at an MOI of 1 for 6 hours at 33°C in EM Medium (120 mM NaCl, 7 mM KCl, 1.8 mM $CaCl_2$, 0.8 mM $MgCl_2$, 5 mM glucose, 25 mM HEPES, pH 7.3). 48 hours after infection cells were stained with Fixable Viability Dye eFluor660 (eBioscience). Cells were then harvested and stained for 1 hour at room temperature with 8 μM CCF4-AM (Invitrogen) in EM medium supplemented with 2.5 μM probenecid. Finally, cells were fixed overnight at 4°C in 4% paraformaldehyde. Cells were analyzed in a LSRFortessa II cytometer using FACSDiva software

(BD Biosciences). At least 50,000 events per sample were collected. Data was analyzed using FlowJo (Treestar, OR).

For inhibition of phagosomal acidification, cells were incubated with 25 nM Bafilomycin A1 (Cambridge Bioscience) and phagosomal permeabilization assay was performed as above. Acidic lysosomes were identified by staining with 100 nM LysoTracker Far Red DND-99 (Molecular Probes) for 30 minutes prior to imaging. Confocal microscopy was performed using a Nikon A1 confocal microscope with a 20x Plan Apo 0.75 NA objective and galvano scanner to generate 10 μm z-stacks consisting of 1 μm optical sections. Data were acquired using NIS Elements version 4.4.

Measuring Bacterial Burden in Larvae

Zebrafish larvae were prepared, infected, and measured for bacterial burden as previously described (Takaki et al., 2013), with the following modifications:

Wild-type two days post-fertilization zebrafish larvae were infected with single-cell suspensions containing approximately 150, 100, and 50 CFU of indicated strains of tdTomato-expressing *M. marinum*. In this experiment, ΔRD1, ΔRD1::WT, and ΔRD1::M93T were infected with 72, 72, and 69 CFU respectively, as quantified by CFU enumeration of injected inoculum. Infected larvae were imaged by fluorescence microscopy at four days post-infection, and resulting images analyzed by fluorescence pixel counting (FPC) to determine bacterial burden. For each larva, total number of fluorescent pixels were quantified using ImageJ, as described previously (Takaki et al., 2013).

Fluorescence microscopy was performed using a Nikon Eclipse Ti-E equipped with a Ti-S-E Motor XY Stage, C-HGFIE 130W mercury light source, 23/0.10 Plan Apochromat objective, and Chroma ET-CY3 (49004) filter cube. Fluorescence images were captured with a Photometrics CoolSNAP HQ2 Monochrome Camera using NIS-Elements (version 3.22). Fluorescence microscopy was performed as previously described (Takaki et al., 2012, 2013).

Visualization of Membrane Disruption by Electron Microscopy

$9x10^9$ CFU of WT or Mm–ΔRD1 in 200 µl PBS were mixed with 125 µl prewashed 20% (v/v) sRBCs in PBS. Samples were mixed and pelleted 5 min at 1000 x *g* on a bed of 5% agarose/PBS, and subsequently incubated at 33°C for 1 hour. 160 µl of supernatant was replaced with 160 µl of ½ Karnovsky's fixative (2% paraformaldehyde, 2.5% glutaraldehyde, 0.2M Cacodylate; Electron Microscopy Sciences) and moved to 4°C. Following overnight incubation, 160 µl supernatant was replaced with 160 µl ½ Karnovsky's fixative 3 times Samples were then transferred to the Fred Hutchinson Electron Microscopy Center for post fixation in 2% OsO_4, dehydration, EPON 812 embedding, ultrathin sectioning, transfer to 200 mesh grids, and post staining with uranyl acetate/lead citrate as described by the Fred Hutchinson Electron Microscopy Procedures Manual (accessible at https://sharedresources.fredhutch.org/training/electron-microscopy-procedures-manual). Samples were imaged on a JEOL 1400 transmission electron microscope and imaged using Gatan digital imaging camera and software. For analysis of membrane disruption, the observer was blinded as to the condition and then imaged 10 randomly selected fields at a magnification of 600x. The number of ghosts and red blood cells were quantified in each field. Each ghost was examined for

membrane disruption. Membrane disruption was scored contact dependent if the disruption occurred within 100 nm of a mycobacterium, and as contact-independent if disruption occurred at a distance greater than 100 nm from a mycobacterium.

Short Term Culture Filtrate Production

Short-term culture filtrates were prepared as previously described (Andersen et al., 1991). In brief, Mm were grown in 7H9 media to OD_{600} >3. The bacteria were then washed and transferred to modified Sauton's medium (0.2 g/L KH2PO4, 0.5 g/L MgSO4.7H2O, 2 g/L Citric Acid, 0.05 g/L ferric ammonium citrate, 60 mL/L glycerol, 4.0 g/L asparagine, pH 7.4), normalized to OD_{600} = 1, and cultured for 48 hours. Bacteria were pelleted at 3220 x *g* for 20 min. Supernatants were collected, filtered through a 0.2-µm filter, supplemented with 1 mM PMSF, and concentrated approximately 200 fold with a Amicon 3kDa centrifugal filter (Merck Millipore). Bacterial pellets were resuspended with 1 mL ice-cold PBS in 1 mM PMSF and lysed with 500 µl of 0.1 mm glass beads (VWR) and lysed by 3x 30 second pulses in a bead beater apparatus. Bacterial debris was separated by centrifugation at 20,000x *g* for 10 min at 4°C and supernatant was collected. The total protein in the culture filtrate and bacterial pellet was quantified using the Pierce BCA protein assay kit (ThermoFisher Scientific). 1 µg protein from culture filtrates and supernatants was separated by SDS-PAGE. Presence of ESAT-6, CFP-10, and GroEL2 was assayed by western blot using the following antibodies: mouse anti-ESAT-6 clone 11G4 (1:1000, Enzo life sciences, BPD-HYB-076-08-02), rabbit anti-CFP-10 (1:500, BEI, product NR13801), mouse anti-GroEL2 clone IT-56 (1:1000, BEI, product NR-13655).

Preparing Single-Cell Suspensions

Single-cell suspensions of mycobacteria were prepared as described by Takaki et al. with minor modifications (Takaki et al., 2013). Briefly, 35 mL mycobacterial cultures were inoculated from glycerol stocks and cultured under kanamycin selection as described above, in Cellstar 250 mL vented tissue culture flasks (Greiner Bio-One, GMBH #658170). Once cultures reached OD_{600} = 0.3-0.6, cultures were pelleted at 3220 x *g* for 20 min at 20°C. Cultures were resuspended in 5 mL middlebrook 7H9 complete media without supplemental tween 80 (7H9 OAD). Samples were passed 10 times through a 27-gauge needle connected to a 10 mL syringe. Passaged cultures were then pelleted at 100 x *g* for 1 minute. 4 mL supernatant was collected. The bacterial pellet was resuspended in 5 mL of 7H9 OAD, and again passed 10 times through a syringe. This process was repeated until 15 mL supernatant was collected. 7.5 mL supernatant was then passed through a 32 mm 5 µm acrodisc syringe filter (Pall #4650) and repeated with the remaining supernatant using a new syringe filter. Filtered supernatant was then centrifuged at 3220 x *g* for 30 min at room temperature. Single-cell pellet was then resuspended in 200 µl 7H9 OAD and divided into 5 µl aliquots and stored at -80°C. Bacterial concentrations (CFU/mL) were determined using the Miles and Misra method (Miles et al., 1938).

Chapter 2 Figures and Tables

Was detergent used in preparation?	Yes		No	
Was phenotype (below) observed?	Yes	No	Yes	No
Lipid bilayer disruption	1[a]	0	0	0
Host cell lysis	6[b]	2[c]	0	3[d]
Liposome disruption	0	0	4[e]	0

Table 2.1. Literature reports of recombinant ESAT-6-mediated lysis parsed by detergent wash step usage in the preparation. Papers that reported recombinant ESAT-6 mediated lysis or membrane disruption were found through a PubMed Search. Whether detergent was used in the ESAT-6 preparation was determined from the Materials and Methods section or from the manufacturer's web site. a, (Hsu et al., 2003), b (Derrick and Morris, 2007; Francis et al., 2014; Kinhikar et al., 2010; Macdonald et al., 2012; Refai et al., 2015; Smith et al., 2008); c, (Hemmati et al., 2016; Wang et al., 2009); d, (Ganguly et al., 2008; Refai et al., 2015; Renshaw et al., 2005); e, (de Jonge et al., 2007; Ma et al., 2015; Peng et al., 2016).

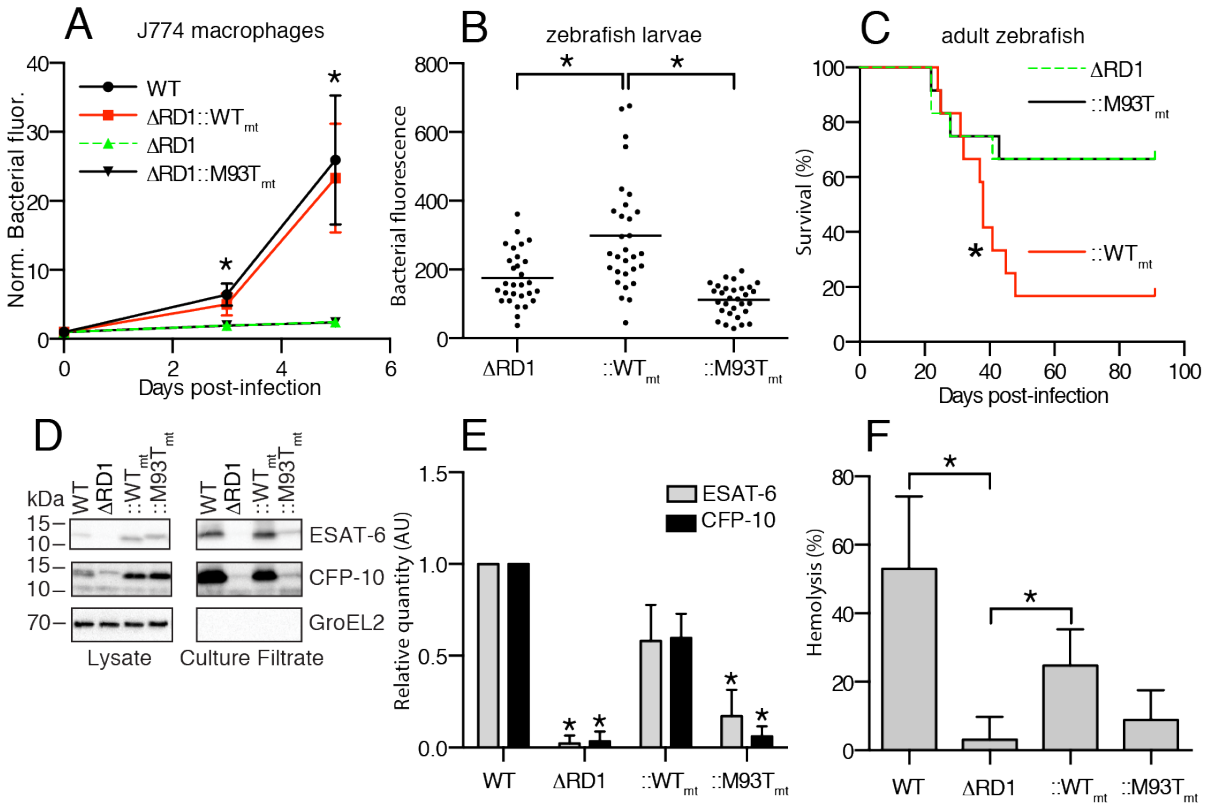

Figure 2.1: Mtb ESX-1 secretion is linked to virulence and hemolysis. (*A*) Bacterial growth in the J774 macrophage cell line as assessed by intracellular bacterial fluorescence. n=12 fields per condition. *p<0.05, two-way ANOVA with Dunnett's test. (*B*) Bacterial burdens in 4 day-post-infection (dpi) zebrafish larvae as assessed by bacterial fluorescence. n=30 larvae per condition. *p<0.05, one-way ANOVA with Dunnett's test. (*C*) Survival of adult zebrafish infected with 100 colony forming units (CFU) of Mm. n=12 fish per condition. *p<0.05, log-rank (Mantel-Cox) test. (*D*) Immunoblot of Mm lysates and culture filtrates. Representative of 4 experimental replicates. (*E*) Protein quantification from (*D*) by image densitometry, relative to WT culture filtrates. *p<0.05, one-way ANOVA with Dunnett's test relative to ::WT. (*F*) Contact-dependent

sheep RBC lysis by $3.0x10^8$ CFU Mm. n=4 experimental replicates. (*E* and *F*) *p<0.05, one-way ANOVA with Dunnett's test relative to ΔRD1. Error bars, SD.

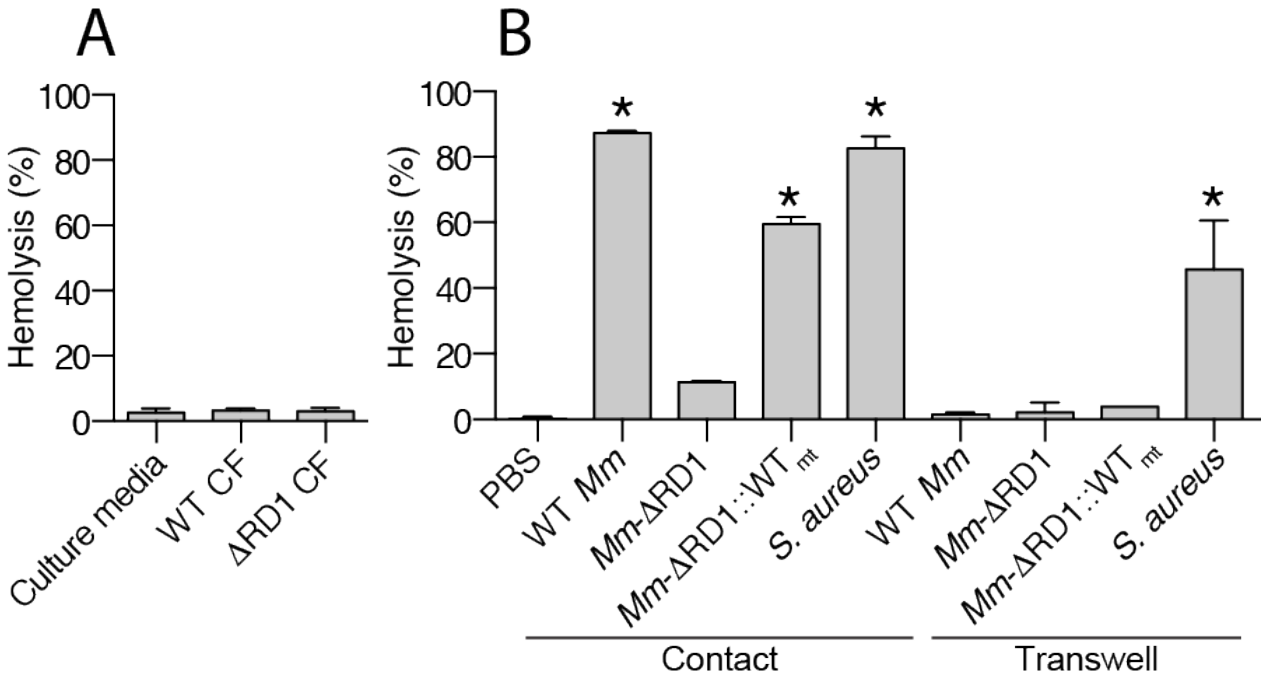

Figure 2.2: ESX-1 dependent hemolysis requires direct contact. (*A*) Hemolysis following addition of culture filtrate from WT Mm, Mm–ΔRD1, or uninoculated media. n=6 experimental replicates. (*B*) Hemolysis following addition of the indicated bacterial strains, either in direct contact with RBCs, or separated by a Transwell. n=3 experimental replicates. *$p<0.05$, one-way ANOVA with Dunnett's test relative to ΔRD1 (contact). Error bars, SD.

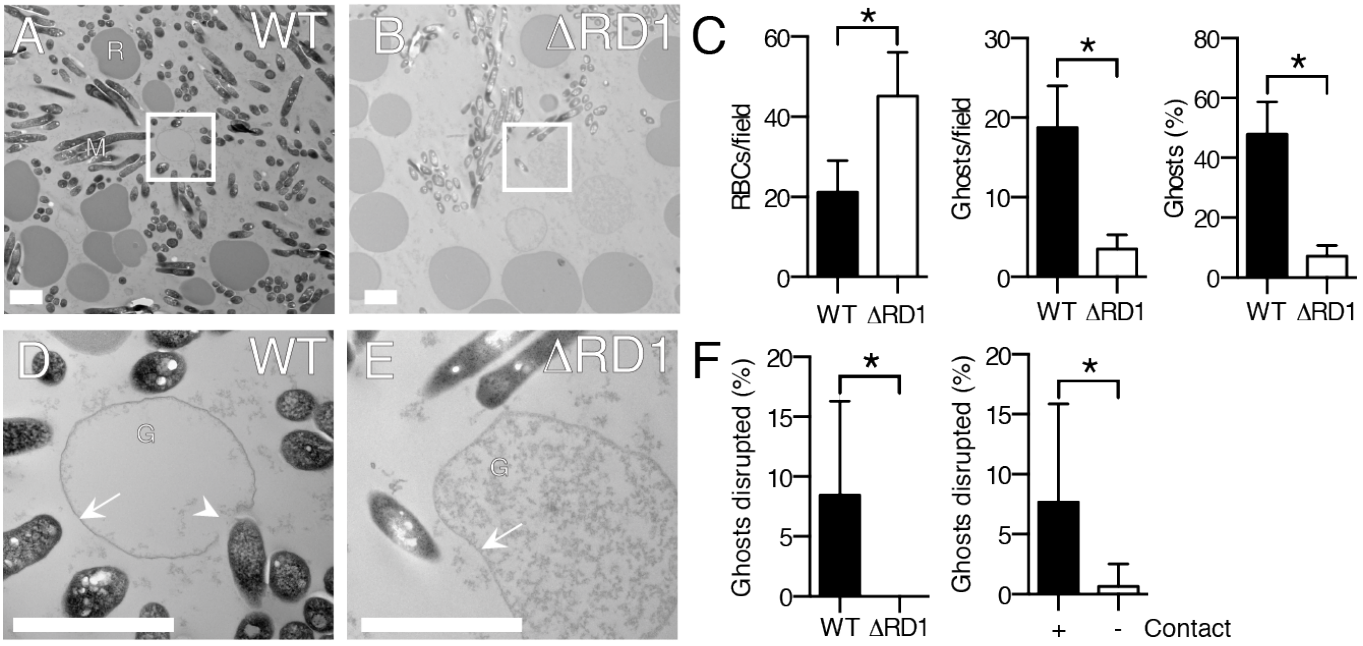

Figure 2.3. ESX-1 dependent hemolysis is accompanied by membrane disruptions at points of bacterial contact without apparent pore formation. (*A* and *B*) Transmission electron micrographs of RBC pellets undergoing contact-dependent hemolysis by WT Mm and Mm–ΔRD1, respectively. R, RBCs; M, Mm. Boxes in A and B indicate the areas magnified in D and E, respectively. (*C*) Total RBCs, lysed ghosts, and lysed ghosts as percentage of total RBCs per field. n=10 fields. (*D* and *E*) Membrane-disrupted ghost in contact with WT Mm (*D*), and intact ghost in contact with Mm–ΔRD1 (*E*). G, ghost; arrow, intact membrane; arrowhead, disrupted membrane. (*F*) Percentage of WT and Mm–ΔRD1 ghosts disrupted per field (left panel), and percentage of contact-dependent or -independent WT ghost disruptions per field (right panel). Scale bar, 2 μm. Error bars, SD. *p<0.05, Student's t-test.

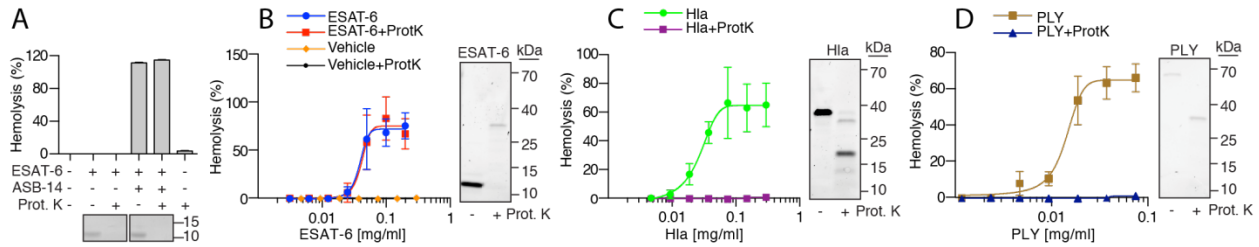

Figure 2.4. Recombinant ESAT-6 lyses host membranes via residual contaminating detergent. (*A*) Lysis of RBCs treated with 0.06 mg/ml rESAT-6 prepared with or without ASB-14, and treated with Proteinase K (Prot. K.). n=3 replicates (top), and Coomassie Blue stained gel of 0.6 µg of corresponding sample (bottom). (*B*) RBC lysis following addition of serially diluted rESAT-6 (BEI) or vehicle ± Prot. K. n=3 experimental replicates (left) and Coomassie Blue stained gel of 1.2 µg protein sample from each condition (right). (*C*, *D*) RBC lysis following addition of serially diluted *S. aureus* α-hemolysin (Hla, ~38 kDa) (*C,* right) or *S. pneumoniae* pneumolysin (PLY, ~70 kDa)(*D,* right), with Coomassie Blue stained gels of 1.2 µg protein on right for each panel

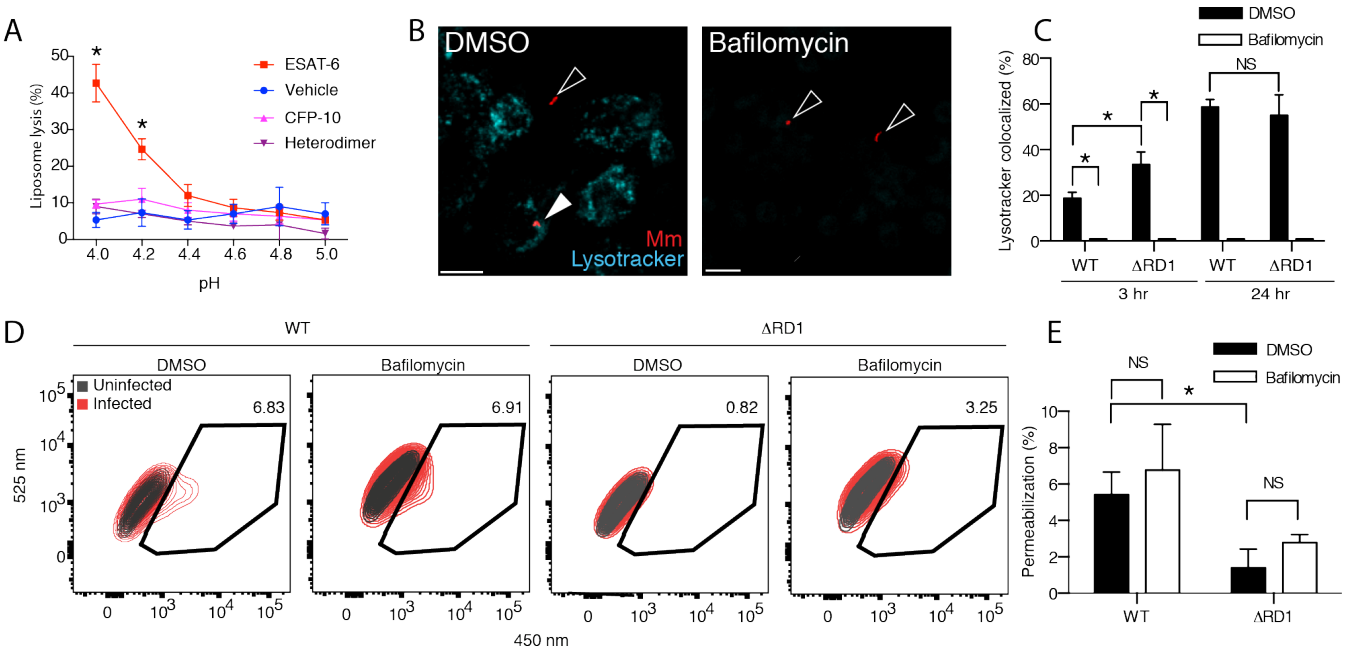

Figure 2.5 Recombinant ESAT-6 lyses membranes at acidic pH**,** while mycobacterial ESX-1-mediated lysis proceeds at neutral pH. (*A*) Quantification of pH-dependent liposome lysis by recombinant ESAT-6, but not CFP-10 or ESAT-6 / CFP-10 heterodimer as measured by fluorescent ANTS release from DOPC liposomes. *p<0.05, two-way ANOVA with Dunnett's multiple comparisons. (*B*) Representative images of THP-1 macrophages infected with WT Mm at 6 hours-post treatment. Scale bar, 20 µm. (*C*) Quantification of co-localization of WT Mm and Mm–ΔRD1 with acidified compartments. n=3 technical replicates. *p<0.05, Mann-Whitney U test. (*D*) Flow cytometry of WT- or ΔRD1-infected THP-1 macrophages. Gate highlights permeabilization events in live, infected macrophages. (*E*) Quantification of permeabilization events. n=3 experimental replicates. Error bars, SD. *p<0.05, one-way ANOVA with Tukey's multiple comparisons test.

Table S2.1. Plasmids used in this manuscript

#	Plasmid	Description	Ref.(s)
1	pTEC31	Mycobacterial plasmid containing the gene for the fluorescent protein tdTomato under the constitutive mycobacterial promoter msp12. Hygromycin plasmid in pTec27 swapped with kanamycin resistance	(Takaki et al., 2013)
2	pYUB412	Empty vector for integration into *attP* site, conferring Hygromycin resistance	(Brodin et al., 2005; Hsu et al., 2003)
3	2F9-EsxA-WT	pYUB412 integrating cosmid containing *M. tuberculosis* RD1 region (bp 4,336,809-4,368,613) between PacI sites. This includes the gene encoding ESAT-6 (*esxA*).	(Brodin et al., 2005; Hsu et al., 2003)
4	2F9-EsxA-M93T	2F9-EsxA integrating cosmid where *EsxA* codon 93 encoding methionine is mutated to threonine (ATG->ACC)	(Brodin et al., 2005)
5	pMRLB.7 – EsxA-His pMRLB.7::EsxA::His	Plasmid for expression and production of recombinant *M. tuberculosis* ESAT-6-6xHis	BEI
6	pMRLB.46 – EsxB-His	Plasmid for expression and production of recombinant *M. tuberculosis* CFP-10-6xHis	BEI
7	pET29 –EsxB-EsxA-His	Bicistronically expressed ESAT-6-6x-His and CFP10. For production of recombinant *M. tuberculosis* ESAT-6/CFP-10 heterodimer	This work
8	pHla-His	Plasmid for expression and production of recombinant *S. aureus* α-hemolysin (Hla)	(Ragle and Bubeck Wardenburg, 2009)
9	pPLY	Plasmid for expression and production of recombinant *S. pneumoniae* Pneumolysin (PLY)	(Lawrence et al., 2015)

Table S2.2. *Mycobacterium marinium* strains used in this manuscript

#	Strain	Description	Antibiotic resistance	Fig.	Ref
1	M strain	WT	None	2.2,2.3	(Ramakrishnan and Falkow, 1994)
2	ΔRD1	M strain with a deleted RD1 locus	None	2.2,2.3	(Volkman et al., 2004)
3	ΔRD1::2F9-EsxA-WT (aka ΔRD1::WT_{mt})	Strain #2 containing plasmid #3. M strain harboring a deleted RD1 locus heterologously expressing the Mtb RD1 locus on an integrating plasmid.	Hygromycin	2.2	This work
4	WT::pYub412+tdtomato	M strain containing the empty vector pYUB412 and the fluorescent protein expressing psmp12::tdtomato vector. Contains plasmids #1 and #2.	Hygromycin, kanamycin	2.1,2.2 ,2.5	This work
5	ΔRD1::pYub412 +tdtomato	ΔRD1 strain containing the empty vector pYUB412 and the fluorescent protein expressing psmp12::tdtomato vector. Contains plasmids #1 and #2.	Hygromycin, kanamycin	2.1,2.2 ,2.5	This work
6	ΔRD1::WT_{mt}+tdtomato (ΔRD1::WT_{mt})	ΔRD1 strain containing the vector pYUB412 harboring the RD1 region of *M. tuberculosis* and the fluorescent protein expressing psmp12::tdtomato vector. Contains plasmids #1 and #3.	Hygromycin, kanamycin	2.1,2.2	This work
7	ΔRD1:: 2F9-ESAT-6^{M93T} +tdtomato (ΔRD1::$M93T_{mt}$)	Same as strain #5, except that it harbors plasmids #1 and #4, expressing EsxA-M93T	Hygromycin, kanamycin	2.1	This work

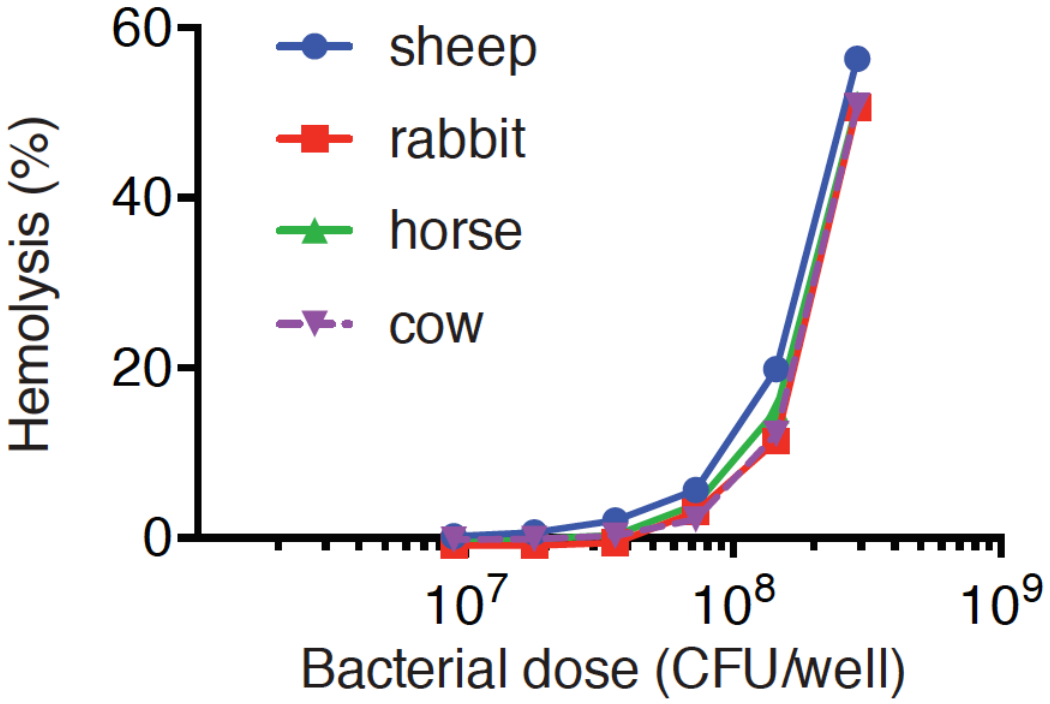

Figure S2.1: No specific difference in mycobacterial lytic activity observed between different species of RBC. $2x10^7$ RBCs of the indicated species were mixed with described concentrations of WT Mm, and contact-dependent hemolysis was measured as described in materials and methods.

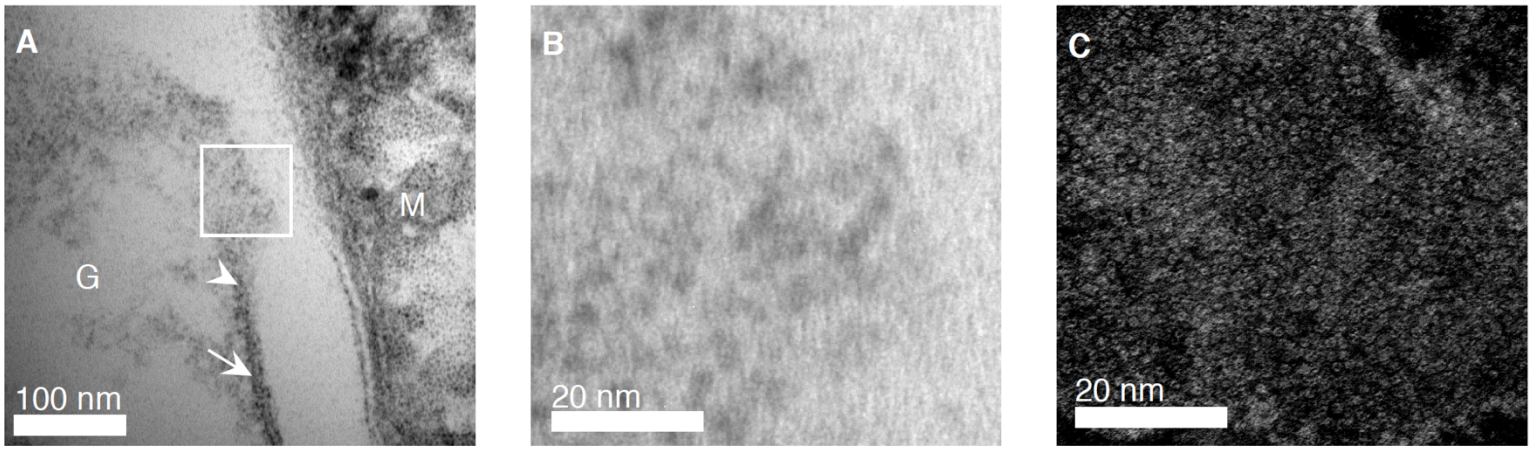

Figure S2.2. No pores detected at point of contact-dependent hemolysis by Mm. (*A*) high resolution electron micrograph (EM) of a sRBC ghost (labeled "G") and WT Mm (labeled "M"). Arrowhead indicates beginning of membrane disruption, while arrow indicates sRBC plasma membrane. Box in (*A*) indicates area of increased magnification depicted in (*B*). No pores observed at highest magnification. (*C*) Example of *S. aureus* Hla pores forming on a RBC membrane as observed by negative stain EM. Reproduced with permission (Freer et al., 1968)

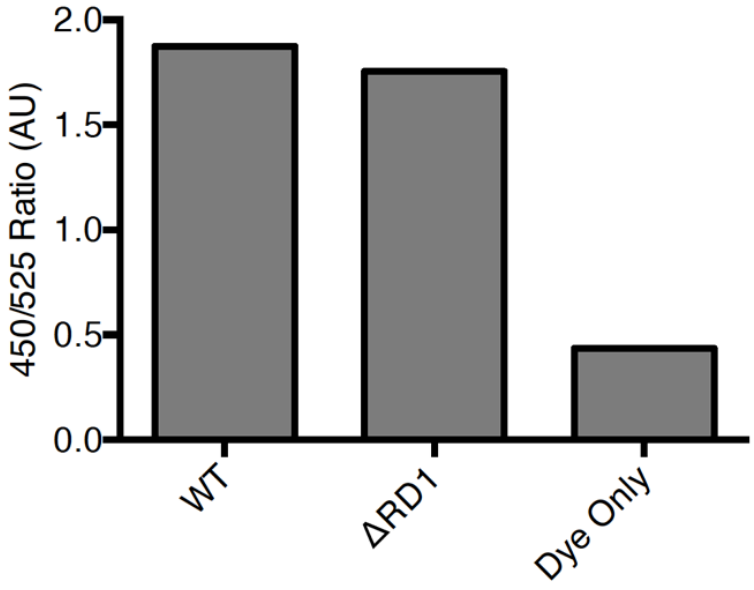

Figure S2.3. WT & RD1 Mm strains show similar *in vitro* lactamase activity as measured by CCF4-AM cleavage. The ratios depicted are values of the 450 nM emission peak divided by the 525nm peak obtained from a 405nm emission scan. Experiment depicts technical triplicate.

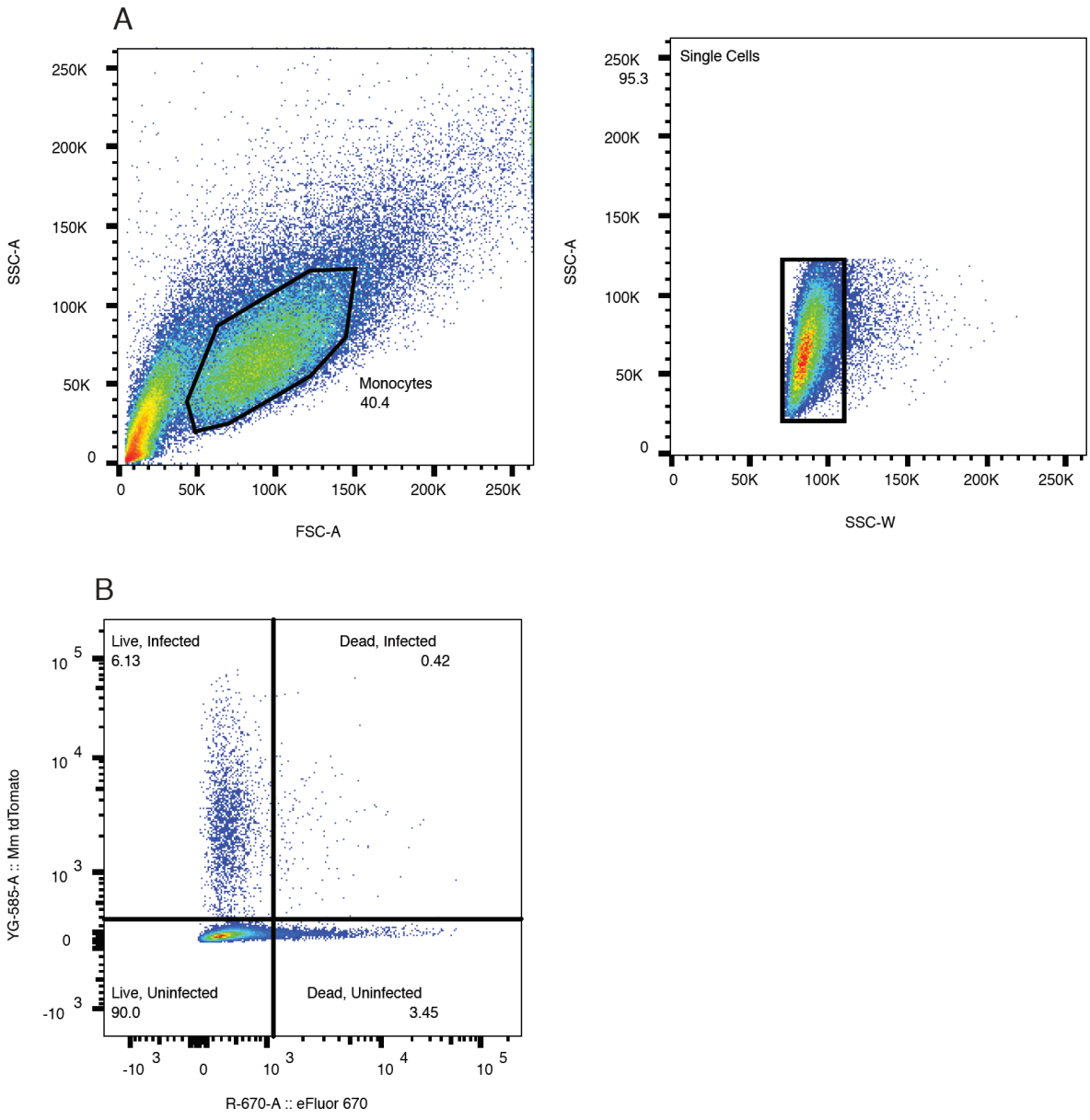
A
SSC-A
FSC-A
Monocytes
40.4
Single Cells
95.3
SSC-W
B
YG-585-A :: Mm tdTomato
R-670-A :: eFluor 670
Live, Infected
6.13
Dead, Infected
0.42
Live, Uninfected
90.0
Dead, Uninfected
3.45

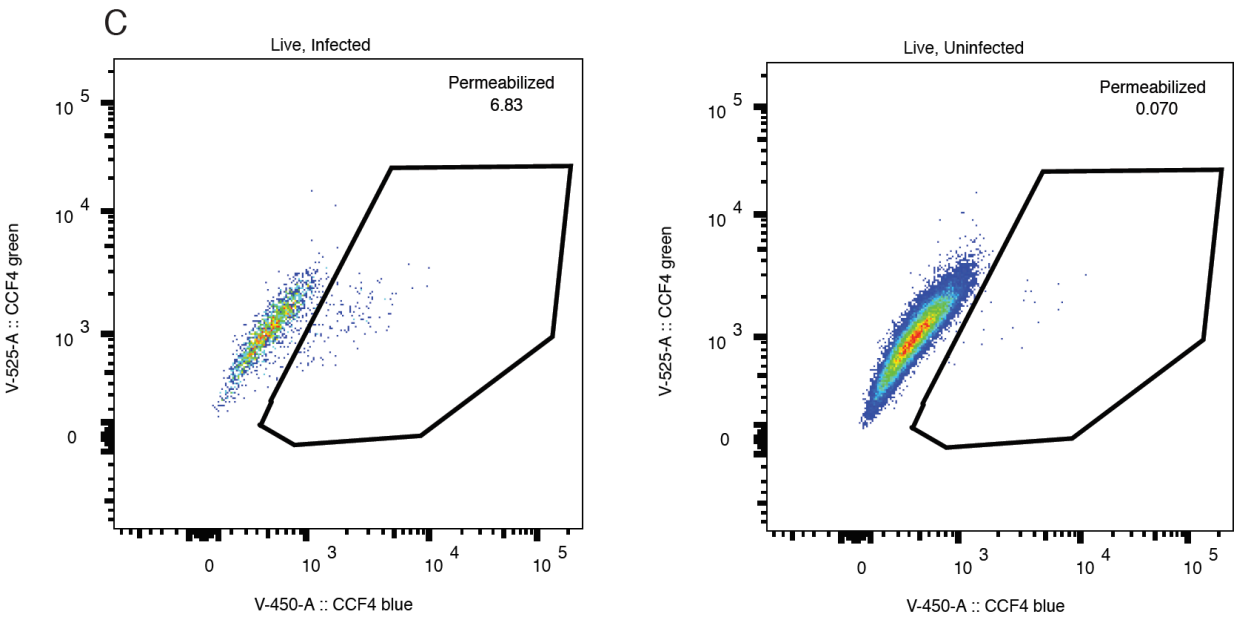

Figure S2.4. Representative flow cytometry gating scheme. (A) FSC-A, forward scatter A; SSC-A, side scatter A; SSC-W side scatter W. Black polygons indicate gated cell subsets. (B) Dotplot showing gating for infected/uninfected cells and live/dead cells based on tdTomato and Fixable Viability Dye eFluor 660 fluorescence. Numbers indicate the percentage of events in respective quadrants. (C) Black polygons indicate region containing permeabilization events. Dot plots are representative of 3 independent experiments.

Chapter 3: Ebselen inhibits ESX-1 mediated secretion and virulence

Summary

The rise of antibiotic resistance threatens to undercut recent successes in combating the spread of tuberculosis, emphasizing the need for the development of new chemotherapies. *Mycobacterium tuberculosis* virulence requires a functional ESX-1 secretion system. Here, I find that the compound ebselen is an inhibitor of ESX-1 secretion. Treatment of *Mycobacterium marinum* with ebselen inhibits ESX-1 secretion and hemolysis without affecting mycobacterial viability. Treatment of infected macrophages with ebselen inhibited ESX-1 mediated growth as well as phagosomal permeabilization. Label-free MS analyses suggest that ebselen treatment inhibits ESX-1 secretion but not that of the paralogous ESX-3 or ESX-5 systems. These data show that ebselen will be a valuable tool for understanding the virulence mechanisms mediated by ESX-1 and may be a potential drug candidate.

Introduction

Despite the development of effective antibiotics over 60 years ago, Tuberculosis (TB) persists as one of world's greatest global health crises. TB afflicts 10 million people annually and kills 1.7 million a year, more than any other infectious disease (World Health Organization, 2017). While TB incidence is slowly dropping (World Health Organization, 2017), this drop is being undercut by a rising tide of antibiotic resistance. In 2016, nearly half a million of multi-drug resistant (MDR) or extensively drug resistant (XDR) TB cases occurred(World Health Organization, 2017), resulting in a quarter million deaths. Treatment of MDR and XDR TB is complex, requiring an 18-24 month drug regimen that only results in successful treatment ~50% of the time (World Health Organization, 2017). Distressingly, totally drug resistant strains have been identified that are untreatable even with the newly discovered drugs bedaquiline and delamanid (Bloemberg et al., 2015). Therefore, the development of new chemotherapies has become a high priority.

The ability of TB to infect its host requires the presence of the Type VII secretion system, ESX-1. ESX-1 was first identified when it was determined that a deletion of the RD1 locus was the primary cause of attenuation for the attenuated live vaccine BCG (Behr et al., 1999; Guinn et al., 2004; Lewis et al., 2003; Mahairas et al., 1996; Pym et al., 2002). Deletion of ESX-1 results in severe attenuation, and complementation of ESX-1 into BCG partially restores virulence (Lewis et al., 2003; Pym et al., 2003). ESX-1 mutants are defective at multiple stages of infection in the pathogenic mycobacteria *Mycobacterium tuberculosis* and *Mycobacterium marinum*: ESX-1 mutants are attenuated in intramacrophage growth (Stanley et al., 2003; Volkman et al., 2004), phagosomal permeabilization (Simeone et al., 2012; van der Wel et al., 2007), granuloma formation (Volkman et al., 2004), and macrophage recruitment (Volkman et

al., 2010). *In vitro,* the ESX-1 locus has been demonstrated to mediate multiple membrane disruption phenotypes, including epithelial cell lysis(Hsu et al., 2003), pneumocyte lysis (Hsu et al., 2003), and hemolysis (Gao et al., 2004; King et al., 1993; Smith et al., 2008). In Chapter 2, I demonstrated that ESX-1 mediated membrane lysis is exclusively contact-dependent, but the mechanism through which ESX-1 lyses host membranes remains unclear. The significance of the ESX-1 locus in establishing and maintaining infection makes it an attractive drug target. Small molecule inhibitors of virulence associated secretion systems has successful for both the type III (Duncan et al., 2012) and type IV secretion systems (Cameron and Zambryski, 2012), reducing both bacterial burden and accelerating clearance (Izoré et al., 2011). *In vitro* screens of ESX-1 mediated phenotypes have been successful in identifying both mutants defective in (Kennedy et al., 2014) and small molecules inhibitors of ESX-1 secretion (Johnson et al., 2015; Rybniker et al., 2014). Using the ESX-1 dependent hemolytic activity of Mm as our readout, I identified the selenium compound ebselen as a specific inhibitor of ESX-1 secretion and virulence associated phenotypes in vitro.

Results

Ebselen is a potent inhibitor of Mm hemolysis at sub-MIC doses.

To identify an inhibitor of ESX-1 activity, I used the contact-dependent hemolytic assay developed by King et al (King et al., 1993) to assess for ESX-1 mediated membrane disruption. I was interested in probing the mechanism of membrane disruption and screened several small molecules to determine if they were capable of inhibiting hemolysis. In this screen, I identified the lipophilic antioxidant Ebselen (Fig. 3.1A) as an inhibitor of hemolytic activity (Fig. 3.1B). Treatment with an inactive analogue of ebselen, DIME (Fig. 3.1A), which lacks the selenium atom that mediates ebselen's antioxidant and cysteine modifying activity (Azad and Tomar, 2014), had no observable effect on hemolysis, suggesting that the inhibitory effect of ebselen is specific to its selenium-mediated activity.

Ebselen has previously been demonstrated to be a broad-spectrum antimicrobial, inhibiting growth at nanomolar concentrations in both gram positive and negative microbes (Thangamani et al., 2015). Antimicrobial activity against Mtb has been observed at doses ranging from 36.4 (Favrot et al., 2013)to 72.8 μM (Lu et al., 2013). To eliminate the possibility that any inhibitory effects I observed were due to ebselen's microbicidal effects during the 2 hours hemolysis assay, I measured OD600 in the presence of 16 μM and 32 μM ebselen in liquid culture. I did not observe any significant growth defects following 4 hours of treatment (Fig. 3.1C). I then formally measured the MICs of ebselen using the standardized resazurin assay on *Mycobacterium marinum*. I determined that the MIC of ebselen to be 100 μM, confirming that the inhibitory effect of 16 μM ebselen was not due to bacterial killing, but an antivirulence effect.

Ebselen inhibits of ESX-1 secretion

Having demonstrated that ebselen was acting as an antivirulence compound, I sought to determine if it was directly inhibiting ESX-1 mediated membrane disruption or ESX-1 secretion. As I observed phenotypic inhibition of ESX-1 activity within 2 hours, I sought to determine whether I could observe depletion of ESAT-6 secretion within a similar time scale. I generated Mm culture filtrates by treating Mm cultures in the presence 32 μM Ebselen, DMSO, or DIME for four hours and harvested the resulting culture supernatants. I found that treatment of Mm with 16 μM ebselen resulted in reduction in the secretion of the ESX-1 substrates EsxA and EsxB within four hours (Fig. 3.2A). This result indicated that ebselen's inhibitory effect was mediated via rapid inhibition of ESX-1 secretion.

To quantify the effect of ebselen on mycobacterial secretion, I prepared short term culture filtrates after four hours of treatment with 32 μM Ebselen (n=3) or DMSO (n=3). Secreted proteins were then quantified using label-free protein quantification with MaxQuant software (Cox et al., 2014), and identified 748 proteins. Curiously, I was unable to observe significant inhibition of ESX-1 secretion (Fig. 3.3B), despite observing reduction of ESAT-6 secretion by immunoblot (Fig 3.1D). I found significant reduction of several proteins, most of which were hypothetical secreted proteins (Table 4.1). None of the hits we observed have been associated with defects in virulence (Sassetti and Rubin, 2003). When I look at ESX-1 substrates identified (EsxA/ESAT-6, EspB, EspE, EspK, and PPE68), I see a noticeable and reproducible reduction in secretion (Fig 3.3B). The ESX-5 substrate EsxG appears also to be downregulated, while the ESX-3 substrate EsxM is slightly upregulated. While these results are tantalizing, it is likely that this experiment was underpowered based on the low protein count. As MaxQuantLFQ sensitivity

is proportional to the amount of identified peptides (Cox et al., 2014), it may be possible to improve our power by running more replicates.

Ebselen inhibits ESX-1 mediated phenotypes at sub-MIC doses.

As I demonstrated in Chapter 2, EsxA secretion corresponds with the ESX-1 mediated phenotypes of hemolysis, intramacrophage growth, and phagosomal permeabilization. As ebselen treatment inhibits secretion of ESX-1 substrates, it would follow that it would affect virulence phenotypes mediated by these substrates. To measure the effect of ebselen on *in vitro* virulence, I infected THP-1 macrophages with fluorescent tdTomato expressing *Mycobacterium marinum*. I then quantified bacterial burden by measuring fluorescence pixel counts (FPC). We found that treatment with both 8 μM and 16 μM ebselen significantly reduced intramacrophage growth (Fig. 3.3A). To confirm that ebselen's effect on intramacrophage growth was ESX-1 specific, ebselen's effect was tested using a *Δerp* Mm mutant, which is attenuated for intramacrophage growth (Cosma et al., 2006). I found that treatment with ebselen and BHT attenuated intramacrophage growth for WT and *Δerp*, but had no significant effect on an ΔRD1 mutant containing a deletion within ESX-1 locus. This confirms that ebselen's effects on virulence are primarily mediated by inhibition of ESX-1 activity.

As ESX-1 function is associated with phagosomal permeabilization(Conrad et al., 2017; Simeone et al., 2012; van der Wel et al., 2007), I sought to test whether treatment with ebselen was capable of inhibiting this phenomenon. I infected activated THP-1 macrophages with tdTomato labeled Mm at an MOI of 1 and treated them with ebselen for 48 hours. Macrophages were then harvested and labelled with the dye CCF-4 to assess for phagosomal permeabilization. I found that treatment with 16 μM ebselen inhibited phagosomal permeabilization in WT infection, while having no effect on the ΔRD1 infection. These experiments include the addition

of BHT, which we originally identified as an inhibitor of membrane disruption. However, this inhibitory effect was minimal compared to ebselen (Fig. 3.S1B). Additionally, both BHT and its inactive analogue, DTBE inhibit hemolysis at nearly identical concentrations (FIG. 3.S1A,C) and neither appear to affect ESX-1 secretion (Fig. 3.S1D). In the future, I plan to repeat these experiments with ebselen treatment alone.

Discussion

This study demonstrates that *in vitro* hemolytic activity may be used as a rapid method for screening for modifiers of ESX-1 activity, identifying ebselen as an inhibitor of a broad range of ESX-1 mediated phenotypes. Ebselen inhibits hemolysis and ESX-1 secretion *in vitro* at doses that do not affect microbial growth. As treatment with the analogue DIME does not inhibit these phenotypes, this suggests that ebselen's activity is mediated by the prescence of a cysteine group. However, as DIME is not a perfect analogue due to its additional methyl groups which could affect substrate affinity. Repeating these experiments with ebsulfur, which contains a less reactive sulfur atom in place of selenium (IMPASE REF), would definitively confirm whether the selenium group mediates this activity.

However, it is most likely that ebselen's inhibitory activity is mediated via seleno-cysteine bond formation. Thi activity has been demonstrated to be required for ebselen's ability to inhibit the Ag85 complex ((Favrot et al., 2014), human inositol monophosphatase(Singh et al., 2013), and its antivirulence effects on *Clostridium difficile* (Beilhartz et al., 2016). Ebselen's antimicrobial properties in Mtb been proposed to be due to interactions with the essential enzyme thioredoxin reductase (Lin et al., 2016). Ebselen has previously been demonstrated to interact with both mammalian and *E. coli* thioredoxins. However, depletion of Mtb thioredoxin had no effect on ebselen's antimicrobial activity (Lin et al., 2016), indicating that its activity is mediated though a separate, unknown mechanism.

Covalent cysteine modification by ebselen has been shown to result in allosteric or active site inhibition of enzymatic activity (Beilhartz et al., 2016; Favrot et al., 2014; Singh et al., 2013). ESX-1 secretion is reliant on the ATPase activity of $EccA_1$, $EccCa_1$, and $EccCb_1$. Mutations in the ATPase domains of $EccA_1$, $EccCa_1$, or $EccCb_1$ abrogate ESX-1 mediated protein secretion (Joshi et al., 2012; Ramsdell et al., 2015). All three proteins contain several

cysteines, some proximal or within ATPase domains. I could determine whether these play a role by doing *in vitro* assessment of the effect of ebselen on enzymatic activity of cysteine point mutants, as has been done for IMPase (Singh et al., 2013)and the Antigen 85 complex (Favrot et al., 2013). Future plans include the use of a biotinylated cysteine modifying probe to identify potential targets using LC/MS, as well as *in vitro* assessment of the effect of ebselen on EccA/C ATPase activity.

Two identified specific inhibitors of ESX-1 secretion have been recently identified: BTP15 (Rybniker et al., 2014) and ethoxzolamide (Johnson et al., 2015). Both inhibitors identified affected ESX-1 secretion through the *espACD* operon, which modulates ESX-1 secretion in Mtb (Bretl et al., 2014; Fortune et al., 2005; Pang et al., 2013). BTP15 was proposed to dysregulate the *espACD* operon through its effects on the MprAB regulon, while Johnson proposes that Ethoxszolamide's inhibiton of ESX-1 secretion is due to its effects on the PhoPR system. Defects in both MprAB and PhoPR affect regulation of the espACD operon, and mutations in either result in defects in ESX-1 secretion. However, *Mycobacterium marinum* mutants in the *espACD* operon, as well as knockouts of *espA* and *phoPR* are still capable of ESAT-6 secretion (Fig S3.1), and an Δ*espA* mutant retains hemolytic activity (data not shown). This demonstrates that ebselen's inhibitory effect on the ESX-1 locus is *espACD* and *phoPR* independent and is likely mediated through a separate mechanism. Identifying ebselen's target is a priority, and importantly, I must verify ebselen's inhibitory effect on Mtb, to ensure that its target is not Mm specific.

In vitro, ebselen presents may provide a useful and effective tool for probing ESX-1 secretion, as it has observable phenotypic effects within 2 hours of treatment (Fig. 3.1B). As ebselen treatment *in vitro* inhibits the virulence phenotypes of intramacrophage growth and

phagosomal permeabilization, confirming the effectiveness in Mtb is critical. Ebselen has been demonstrated to be clinically safe and well tolerated in humans (Kil et al., 2017; Yamaguchi et al., 1998). Given the pressing need for new TB therapies, I believe that ebselen is a promising candidate for drug repurposing.

Experimental Procedures

Bacterial strains

All strains were derived from *Mycobacterium marinum* (Mm) strains purchased from American Type Culture Collection (ATCC) (strain M, ATCC no. BAA-535). RD1-deleted Mm (ΔRD1) and RD1 complement Mm strains were generated as described in Chapter 2.

MIC Assays

MICs were measured in liquid medium using a resazurin assay. 100 µL of bacteria were diluted to an OD600 of 0.01 in 7H9 medium, and grown in the presence of 2-fold serial dilutions of antibiotic for 96 hours at 33°C. 100 µL of 0.01% resazurin was added and cells were incubated for an additional day. MIC was defined as the lowest concentration of drug that prevented a change in color from pink to blue.

Hemolysis assays

Hemolysis was performed as described in Chapter 2. For treatments, drug (BHT/EBS) or vehicle (EtOH/DMSO) was added immediately prior to addition of washed sRBCs.

Secretion Assays

Briefly, 70 mL of Mm was grown from an initial OD of 0.01 to an OD600 of 1.5-2.0 in 7H9 Complete Medium. At this point, hemolytic activity was tested to ensure that the cultures were ESX-1 competent. Cultures were then washed twice in PBS and transferred to Sautons Medium. Ebselen (Sigma), 2-(2,6-dimethylphenyl)-1-isoindolinone (Sigma), or DMSO was then added and the cultures were allowed to grow for 4 hours at 33°C. Bacteria were pelleted at 3220 x g for 20 min. Supernatants were collected, filtered through a 0.2-µm filter, supplemented with 1 mM PMSF, and concentrated approximately 700 fold with a Amicon 3kDa centrifugal filter (Merck Millipore). Bacterial pellets were resuspended with 1 mL ice-cold PBS in 1 mM PMSF and lysed

with 500 µl of 0.1 mm glass beads (VWR) and lysed by 3x 30 second pulses in a bead beater apparatus. Bacterial debris was separated by centrifugation at 20,000x g for 10 min at 4°C and supernatant was collected. The total protein in the culture filtrate and bacterial pellet was quantified using the Pierce BCA protein assay kit (ThermoFisher Scientific). 1 µg protein from culture filtrates and supernatants was separated by SDS-PAGE. Presence of ESAT-6 and GroEL2 was assayed by western blot using the following mouse anti-ESAT-6 clone 11G4 (1:1000, Enzo life sciences, BPD-HYB-076-08-02) and mouse anti-GroEL2 clone IT-56 (1:1000, BEI, product NR-13655) respectively.

Measuring phagosomal permeabilization

Phagosomal permeabilization was measured and scored using he β-lactamase CCF-4 FRET assay as described in Chapter 2. Briefly, 72 hours prior to infection, THP-1 macrophages were stimulated with 33 nM phorbol 12-myristate 13-acetate (Sigma) and plated at $6x10^5$ cells/mL. Activated THP-1s were infected with single-cell suspensions of tdTomato labelled Mm (66) at an MOI of 1 for 6 hours at 33°C in EM Medium in the presence of 16 uM Ebselen (Sigma) or DMSO (Sigma). Following infection cells were washed with PBS and then incubated for 48h in EM Medium with 10% FCS in the presence of 16 uM ebselen or DMSO.

Cells were then washed with warm PBS and then stained with Fixable Viability Dye eFluor660 (eBioscience). Cells were then harvested using Accutase (Sigma) and then stained with 8 µM CCF4-AM (Invitrogen) in EM medium supplemented with 2.5 µM probenecid, and then fixed overnight at 4°C in 4% paraformaldehyde. Cells were analyzed in a LSRFortessa II cytometer using FACSDiva software (BD Biosciences). At least 50,000 events per sample were collected. Data was analyzed using FlowJo (Treestar, OR).

Trypsin digestion

Protein samples were reduced with 10 mM DTT at 56 °C for 30 min and alkylated with 15 mM iodoacetamide in the dark at room temperature (RT) for 30 min. The alkylation reaction was quenched by the addition of 5mM DTT at RT for 10 min and the samples were digested with trypsin (Promega, 0.5ug) over night at 37°C. Digested peptide mixtures were then acidified, partially dried down in a SpeedVac concentrator (Savant) and desalted using a home-made C18 (3M Empore) stage tip filled with 0.5 mg of Poros R3 (Applied Biosystems) resin. Bound peptides were eluted with 30-80% acetonitrile in 0.1%TFA and partially dried to prepare for LC-MSMS.

LC-MSMS

Peptides were analyzed on a Q Exactive Plus hybrid quardrupole-Orbitrap mass spectrometer (Thermo Fisher Scientific). Liquid chromatography was performed on a fully automated Ultimate 3000 RSLC nano System (Thermo Scientific) fitted with a 100µm x 2cm PepMap100 C18 nano trap column and a 75µm×25cm reverse phase C18 nano column (Aclaim PepMap, Thermo Scientific). Samples were separated using a binary gradient consisting of buffer A (2% MeCN, 0.1% formic acid) and buffer B (80% MeCN, 0.1% formic acid). Peptides were eluted with a steps gradient from 4 to 30% buffer B in 75 min and 30-50% B in 12 min with a flow rate 300 nl/min. The eluted peptides were sprayed directly into a Q Exactive Plus mass spectrometer (Thermo Scientific) via a nanospray ion source. The mass spectrometer was operated in standard data dependent mode, performed survey full-scan (MS, m/z = 350-1600) with a resolution of 35000, followed by MS2 acquisitions of the 15 most intense ions with a resolution of 17500 and NCE of 27%. MS target values of 3e6 and MS2 target values of 1e5 were used. Dynamic exclusion was enabled for 30s.

MS data analysis

The acquired MS-MS raw files were processed using MaxQuant (Cox et al., 2014) with the integrated Andromeda search engine (v.1.5.5.1). MSMS spectra were searched against the *Mycobacterium marinum* UniProt FASTA database (2016). The search parameters included cysteine carbamidomethylation as a fixed modification and N-acetylation of protein, oxidation of methionine, and conversion of Gln to pyro-Glu as variable modifications. Enzyme specificity was set to trypsin, and up to two missed cleavages were allowed for protease digestion. Parameters used for label free quantification was LFQ min ratio count of 1, match between runs and others as default values. MaxQuant output was processed with Perseus software (v 1.5.5.0)(Tyanova et al., 2016). After uploading the LFQ intensities, data was filtered to remove identifications from reverse database, common contaminants and only identify by modified peptides. LFQ intensities were log2 transformed, filtered to keep minimum present in 3 replicates in total and missing values were imputed with values around the detection limit. For ANOVA analysis, replicates were grouped and performed the statistical test with permutation-based false discovery rate (FDR) of 0.05. Hierarchical clustering of proteins were carried out on ANOVA significant hits only.

Chapter 3 Figures and Tables

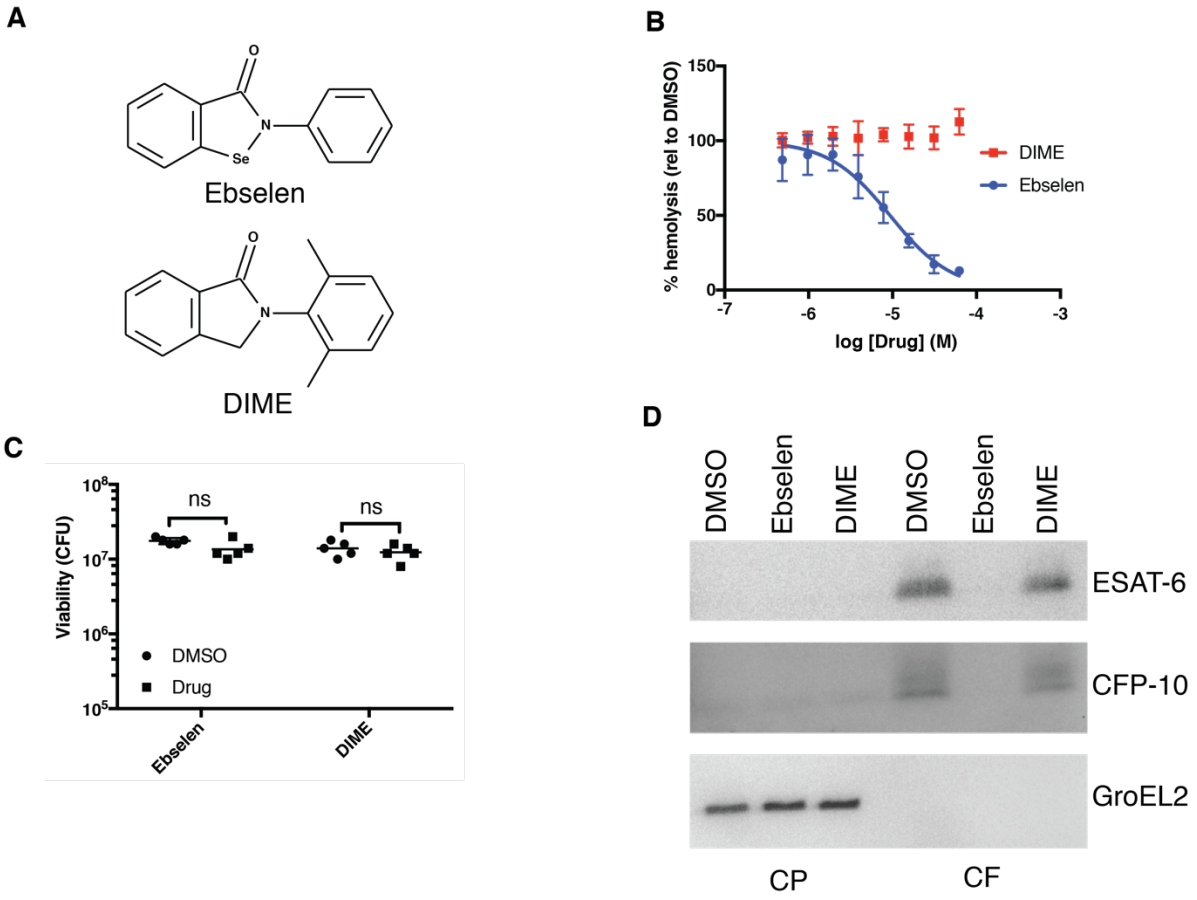

Figure 3.1. Ebselen inhibits hemolysis and ESX-1 secretion in *Mycobacterium marinium.* (A) Depiction of Ebselen, and its inactive analogue DIME, which lacks the selenium atom which mediates its activity. (B) Treatment with 16 µM ebselen inhibits ESX-1 mediated hemolysis in *Mycobacterium marinum.* Experiment is representative of three independent replicates. (C) 16 µM Ebselen treatment does not significantly affect *in vitro* growth. 2-way ANOVA. (D) 4 hour treatment with 32 µM ebselen, but not DIME, inhibits secretion of the ESX-1 substrates ESAT-6 and CFP-10. Experiment is indicative of three independent replicates. ns: $p>0.05$.

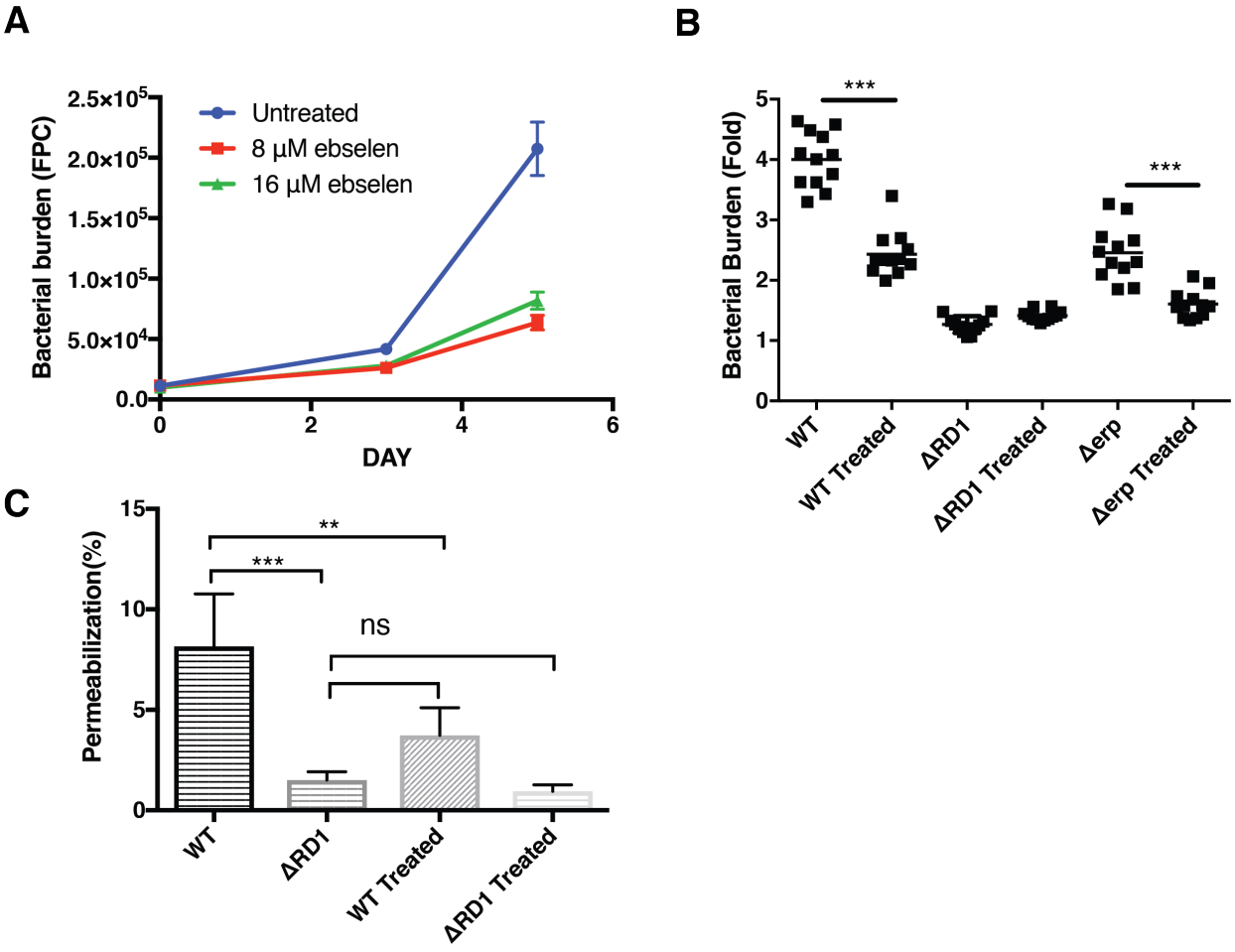

Figure 3.2. Ebselen treatment inhibits intramacrophage growth and phagosomal permeabilization. (A) Treatment of infected J774 macrophages with 8 and 16 µM ebselen inhibits intramacrophage growth. Experiment is representative of three independent experiments. (B) Treatment of infected J774s with 16 µM Ebselen + 78 µM BHT inhibits intramacrophage growth in WT and *erp,* but not in RD1. (C) Treatment of infected THP-1s with Ebselen/BHT combo inhibits phagosomal permeabilization. Results are compiled from 3 independent experiments. Error bars, SD. *p< .05, One-way ANOVA. ns, p>0.05.

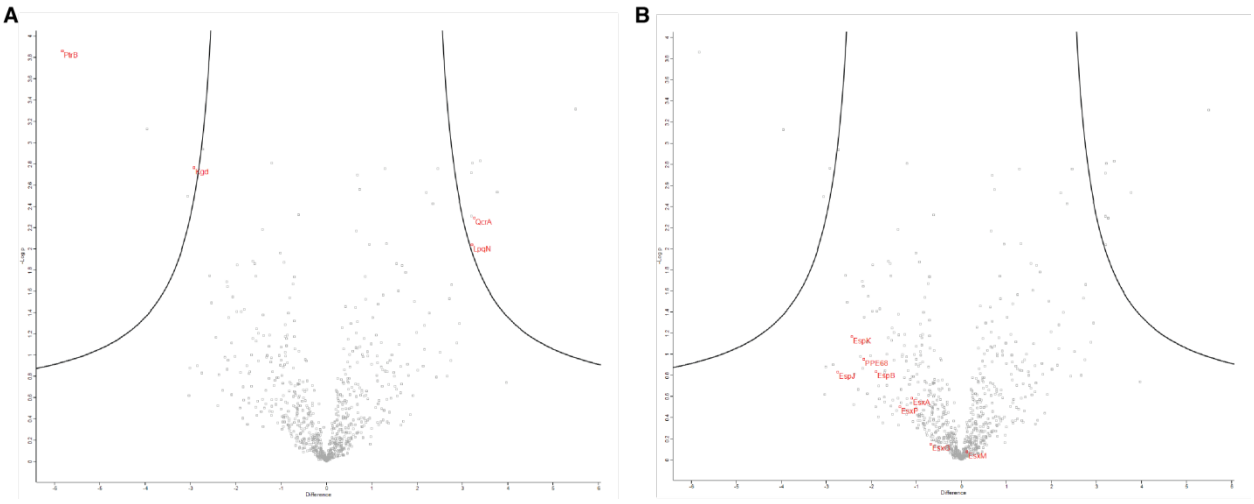

Figure 3.3. LFQ intensity differences of culture filtrates generated from ebselen compared to DMSO. (A) Volcano plot highlighting non-hypothetical proteins with homologs in Mtb (PtrB, Kgd, QcrA, LpqN) that are significantly up or downregulated following ebselen treatment (B) Highlighting of ESX-1, ESX-3, and ESX-5 substrates identified. Volcano plots were generated by Persesus. Three biologically independent replicates were grouped, and statistical tests with a permutation-based false discovery rate (FDR) of 0.05. X axis is the difference between LFQ intensities between Ebselen and DMSO treatments, while Y axis corresponds to the negative log of the p value.

Table 3.1. Significant Hits from Label-Free Quantification.

Difference	UniProt	Protein Name	UniProt Submitted Name
-5.83	B2HH57	PtrB	Protease II (Oligopeptidase B), PtrB
-3.95	B2HK65	MMAR_5156	Conserved Hypothetical Protease
-3.06	B2HLL1	MMAR_5339	PE-PGRS family protein
-2.92	B2HRH1	Kgd	Alpha-ketoglutarate decarboxylase Kgd
-2.73	B2HEE3	MMAR_4562	PE-PGRS family protein
2.45	B2HFS2	MmpS4_1	Conserved membrane transport protein, MmpS4_1
3.20	B2HT31	MMAR_4345	Conserved hypothetical exported protein
3.20	B2HKC4	MMAR_5216	Conserved hypothetical secreted protein
3.21	B2HSE9	LpqN	Conserved lipoprotein, LpqN
3.22	B2HQ12	MMAR_2306	Uncharacterized protein
3.26	B2HGW3	QcrA	Rieske iron-sulfur protein QcrA
3.39	B2HIU5	MMAR_3427	PE Family Protein
3.76	B2HDV1	MMAR_1209	Uncharacterized protein
5.49	B2HRQ4	MMAR_0909	Methyltransferase

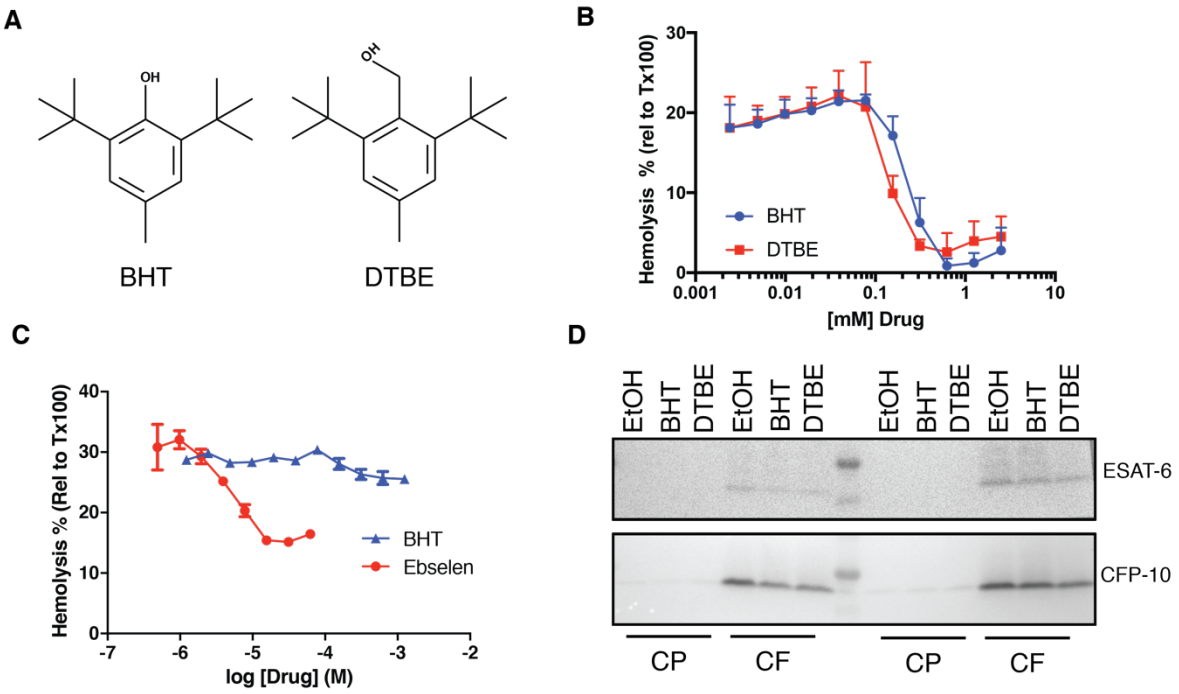

Figure S3.1. BHT inhibits hemolytic activity but does not affect ESAT-6 secretion. (A) Chemical structures of BHT and its inactive analogue DTBE. (B) Both BHT and DTBE inhibit hemolysis at similar doses, suggesting that BHT's inhibition is not specific to its antioxidant activity. (C) Ebselen is a more effective inhibitor of hemolysis than BHT. Error bars, SD. (D) 4 hour treatment with 40 μM BHT and DTBE is not sufficient to reduce secretion of ESAT-6 or CFP-10 into culture filtrates. CP – Cell pellet, CF – culture filtrate.

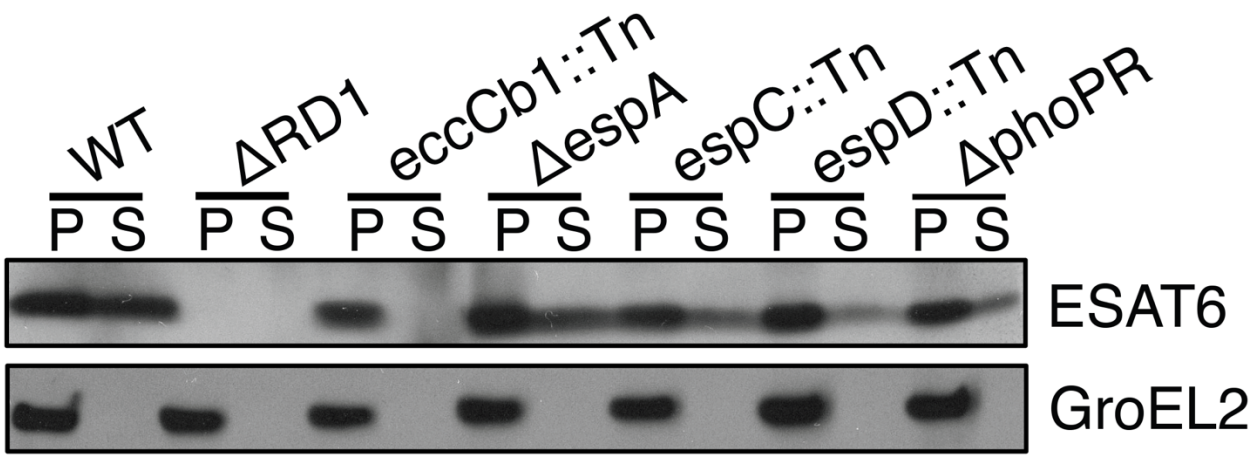

Figure S3.2. ESAT-6 Secretion in Mycobacterium Marinum is not dependent upon PhoPR or *espACD.* (A) Chemical structures of BHT and its inactive analogue DTBE. (B) Both BHT and DTBE inhibit hemolysis at similar doses, suggesting that BHT's inhibition is not specific to its antioxidant activity. (C) Ebselen is a more effective inhibitor of hemolysis than BHT. Error bars, SD. (D) 4 hour treatment with 40 μM BHT and DTBE is not sufficient to reduce ESAT-6 secretion. P – Cell pellet. S – Culture supernatant.

Chapter 4: Concluding Thoughts

Since its determination as the primary means of attenuation of BCG, understanding the function of the ESX-1 secretion system in *Mycobacterium tuberculosis* has become one of the most studied topics in the TB field. While the initial discovery of Mtb's membrane disrupting activity was observed in 1993, it was only until ten years later when Hsu et al proposed that ESX-1 was secreting a lysin that this activity was associated with virulence. The subsequent publication of Smith showing that Mm disruption of erythrocytes could be recapitulated using purified ESAT-6 solidified the hypothesis that ESAT-6 was acting as a pore forming toxin (Smith et al., 2008), supporting its role as the primary mediator of ESX-1 virulence. I propose that this hypothesis continued to prevail due to two primary factors: 1) The confounding due to the interdependence of ESX-1 substrate secretion (Champion et al., 2014; Fortune et al., 2005) and 2) misleading results caused by the unintentional use of detergent contaminated ESAT-6. I demonstrate in this work that ESX-1's membrane disrupting activity is exclusively contact dependent and not due to ESAT-6 independently acting as a secreted lysin.

In light of this evidence, it is more likely that studies discussing the primacy of ESAT-6 virulence were demonstrating the importance of ESX-1 secretion. We are nearly as clueless about the mediators of membrane disruption as we were ten years ago, when van der Wel and colleagues demonstrated that ESX-1 mediated phagosomal permeabilization and cytosolic translocation(van der Wel et al., 2007). But if we go back to those images they presented, we are provided with some mechanistic hints. The gross tears that we observed in Mm-disrupted erythrocyte ghosts (Fig. 2.3D) appear similar to those observed following ESX-1 mediated phagosomal disruptions of myeloid cells (Houben et al., 2012a; van der Wel et al., 2007). When we extend our observations to other intracellular pathogens, we find similarity to those mediated

by Phospholipase A2 in *Rickettsia spp* (Walker et al., 2001). While mycobacterial phospholipases do not appear to play a role in phagosomal permeabilization (Le Chevalier et al., 2015), *in vitro* membrane disruption has also been associated with the acid sphingomyelinase SpmT (Speer et al., 2015). Speer and colleagues do observe that SpmT is not responsible for all of Mtb's hemolytic activity, but it may be possible that SpmT is one of a combination of factors involved in membrane disruption, much as *Listeria monocytogenes'* hemolysin Listeriolysin O works in concert with other phospholipases to escape its intracellular vacuole (Alberti-Segui et al., 2007).

While contact dependence is required for membrane disruption, it does not exclude the possibility that membrane disruption is mediated by an ESX-1 substrate. An ESX-1 substrate may require an unknown post-translational modification to become a lysin. *Serratia marcescens* ShlA hemolysin must be activated by its partner ShlB in order to mediate membrane disrupting activity(Walker et al., 2004). Alternatively, expression of a lysin could be tightly regulated and only induced following contact with a host membrane, which could be mediated by an ESX-1 dependent surface complex. Analysis of Mtb capsule extracts identified several ESX-1 substrates (Sani et al., 2010), and ESX-5 mutants that disrupt capsule integrity inhibit ESX-1 mediated membrane disruption (Ates et al., 2015). The capsule-bound ESX-1 substrate EspC polymerizes to form filaments *in vitro,* and that these filaments can be observed on the mycobacterial capsule (Lou et al., 2017). Mutations that inhibit polymerization of EspC abrogate ESAT-6 secretion (Lou et al., 2017). The authors hypothesize that EspC's polymerization may be similar to polymeric components of the type II, III, or IV secretion systems, suggesting that EspC may be one component of a larger secretory complex.

We still do not know how ESX-1 substrates are secreted extracellularly by mycobacteria, as the core components of the ESX-1 locus rest solidly in the mycobacterial inner membrane. Mycobacteria have a unique diderm membrane architecture containing an inner plasma membrane and mycomembrane separated by a 20nm periplasmic space (Sani et al., 2010) (Fig. 4.1). The mycomembrane differs in composition from the LPS-rich gram negative outer membranes, and is made up of covalently linked layers of peptidoglycans, arabinoglycans, and mycolic acids. Resting on the surface of the mycomembrane is the cell capsule, consisting of an array of polysaccharides and bound proteins. Spanning the mycomembrane and capsule are porins that are associated with nutrient uptake, however, associations between membrane porins and ESX-1 substrates have yet to be observed (Niederweis et al., 2010). How ESX-1 substrates traverse this complex membrane remains one of the most pressing mysteries of the field.

Two recent studies have suggested that the mycobacterial cell wall lipid phthiocerol dimycocerosate (PDIM) may contribute to phagosomal permeabilization (Augenstreich et al., 2017; Quigley et al., 2017). Quigley and colleagues found that a transposon mutant of MmpL7, which transports PDIM from the mycobacterial cytosol to the outer membrane, was found to be deficient in phagosomal permeabilization. This result was independently verified by Augenstreich J and colleagues, which found that deletion of the *mas* gene, which encodes a mycocerosic acid synthase required for PDIM production, showed similar defects (Augenstreich et al., 2017). These defects were found to be independent of ESX-1 secretion in both studies. Both groups propose that PDIM may enhance membrane disruption by inserting into and changing the biophysical properties of host membranes. Alternatively, given the recent discovery of EspC filaments on the cell capsule(Lou et al., 2017), it may be possible that PDIM production

is required for proper assembly or function of an extracellular ESX-1 complex that assembles upstream of ESX-1 secretion.

Despite being the most intensely studied of ESX-1 substrates, there is little known about ESAT-6's biochemistry beyond its interaction with CFP-10. EspA interacts with EspC, and is thought to be involved in shuttling EspC to the cell envelope (Lou et al., 2017). CFP-10/EsxB thought to be merely a chaperone for ESAT-6, directly interacts with the $EccCb_1$ portion of the ESX-1 translocon. This interaction was shown to be critical for both translocon assembly and activity through this interaction (Rosenberg et al., 2015). Finally, a recent EM structure of EspB produced a heptameric complex with a large central channel, suggesting it may play a role in substrate transport or host interaction (Solomonson et al., 2015).

We are left with as nearly as many questions as when we started. There are many tantalizing clues to the function of ESX-1 secretion, yet we lack a cohesive picture. We still do not understand why membrane disruption is contact dependent, nor do we know how substrates are shuttled through the periplasmic space and mycobacterial outer membrane. We still have a poor understanding of the function of ESX-1 and its substrates at the biochemical and structural level. Are ESX-1 substrates directly involved in membrane disruption, or are they structural components of the mycobacterial capsule? Why are such antigenic substrates secreted in vast quantities into the extracellular space?

Jean-Antoine Villemin's first presented his discovery of tuberculosis as an infectious disease in 1867, 151 years ago (Daniel, 2015). *Mycobacterium tuberculosis* has co-evolved with humanity for tens of millennia, and in this time it developed mechanisms to combat human immune responses at nearly every step of infection (Cambier et al., 2014). Given that we have had a relatively short span of clumsily probing the bacillus' biology, it is unsurprising that there

remain so many remaining mysteries. But with continued perseverance and the development of iteratively slightly less clumsy tools, it may be possible to build a complete understanding of the host-pathogen interplay that underlies *Mycobacterium tuberculosis*' pathogenesis.

Chapter 4 Figures

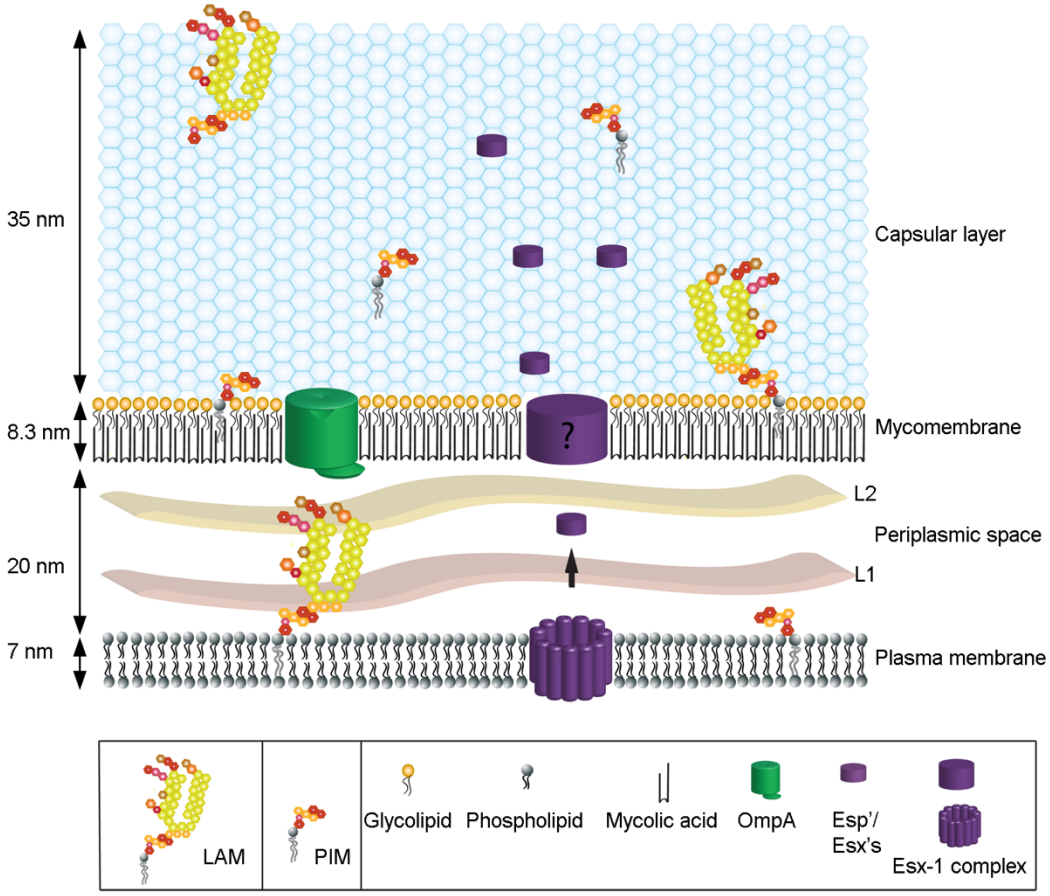

Figure 4.1. Organization of the mycobacterial cell envelope. Left, relative size of each component. LAM – lipoarabinomannan, PIM - phosphatidylinositol mannoside, OmpA - outer membrane porin. L2 and L1 correspond to possible polysaccharide layers identified in the perplasmic space. Originally published in (Sani et al., 2010), and licensed under the Creative Commons Attribution license.

References

Abdallah, A.M., Verboom, T., Weerdenburg, E.M., Gey van Pittius, N.C., Mahasha, P.W., Jiménez, C., Parra, M., Cadieux, N., Brennan, M.J., Appelmelk, B.J., et al. (2009). PPE and PE_PGRS proteins of Mycobacterium marinum are transported via the type VII secretion system ESX-5. Mol. Microbiol. *73*, 329–340.

Alberti-Segui, C., Goeden, K.R., and Higgins, D.E. (2007). Differential function of Listeria monocytogenes listeriolysin O and phospholipases C in vacuolar dissolution following cell-to-cell spread. Cell. Microbiol. *9*, 179–195.

Andersen, P., Askgaard, D., Ljungqvist, L., Bennedsen, J., and Heron, I. (1991). Proteins released from Mycobacterium tuberculosis during growth. Infect. Immun. *59*, 1905–1910.

Andersen, P., Andersen, a B., Sørensen, a L., and Nagai, S. (1995). Recall of long-lived immunity to Mycobacterium tuberculosis infection in mice. J. Immunol. *154*, 3359–3372.

Ates, L.S., Ummels, R., Commandeur, S., van de Weerd, R., van der Weerd, R., Sparrius, M., Weerdenburg, E., Alber, M., Kalscheuer, R., Piersma, S.R., et al. (2015). Essential Role of the ESX-5 Secretion System in Outer Membrane Permeability of Pathogenic Mycobacteria. PLoS Genet. *11*, e1005190.

Ates, L.S., van der Woude, A.D., Bestebroer, J., van Stempvoort, G., Musters, R.J.P., Garcia-Vallejo, J.J., Picavet, D.I., Weerd, R. van de, Maletta, M., Kuijl, C.P., et al. (2016). The ESX-5 System of Pathogenic Mycobacteria Is Involved In Capsule Integrity and Virulence through Its Substrate PPE10. PLoS Pathog. *12*, e1005696.

Augenstreich, J., Arbues, A., Simeone, R., Haanappel, E., Wegener, A., Sayes, F., Chevalier, F. Le, Chalut, C., Malaga, W., Guilhot, C., et al. (2017). ESX-1 and phthiocerol dimycocerosates of *Mycobacterium tuberculosis* act in concert to cause phagosomal rupture and host cell apoptosis. Cell. Microbiol. 1–19.

Azad, G.K., and Tomar, R.S. (2014). Ebselen, a promising antioxidant drug: mechanisms of action and targets of biological pathways. Mol. Biol. Rep. *41*, 4865–4879.

Bach, H., Papavinasasundaram, K.G., Wong, D., Hmama, Z., and Av-Gay, Y. (2008). Mycobacterium tuberculosis virulence is mediated by PtpA dephosphorylation of human vacuolar protein sorting 33B. Cell Host Microbe *3*, 316–322.

Beckham, K.S.H., Ciccarelli, L., Bunduc, C.M., Mertens, H.D.T., Ummels, R., Lugmayr, W., Mayr, J., Rettel, M., Savitski, M.M., Svergun, D.I., et al. (2017). Structure of the mycobacterial ESX-5 type VII secretion system membrane complex by single-particle analysis. Nat. Microbiol. *2*, 17047.

Behr, M.A., Wilson, M.A., Gill, W.P., Salamon, H., Schoolnik, G.K., Rane, S., and Small, P.M. (1999). Comparative genomics of BCG vaccines by whole-genome DNA microarray. Science *284*, 1520–1523.

BEI Resources (2009). Production of Recombinant ESAT-6 Under Non-Denaturing Conditions SOP.

Beilhartz, G.L., Tam, J., Zhang, Z., and Melnyk, R.A. (2016). Comment on A small-molecule antivirulence agent for treating Clostridium difficile infection. Sci. Transl. Med. *8*, 8–11.

Berthet, F.-X.X., Lagranderie, M., Gounon, P., Laurent-Winter, C., Ensergueix, D., Chavarot, P., Thouron, F., Maranghi, E., Pelicic, V., Portnoï, D., et al. (1998). Attenuation of Virulence by Disruption of the Mycobacterium tuberculosis erp Gene. Science (80-.). *282*, 759–762.

Bitter, W., Houben, E.N.G., Bottai, D., Brodin, P., Brown, E.J., Cox, J.S., Derbyshire, K., Fortune, S.M., Gao, L.-Y., Liu, J., et al. (2009). Systematic genetic nomenclature for type VII

secretion systems. PLoS Pathog. *5*, e1000507.
Bloemberg, G. V, Keller, P.M., Stucki, D., Stuckia, D., Trauner, A., Borrell, S., Latshang, T., Coscolla, M., Rothe, T., Hömke, R., et al. (2015). Acquired Resistance to Bedaquiline and Delamanid in Therapy for Tuberculosis. N. Engl. J. Med. *373*, 1986–1988.
Boritsch, E.C., Supply, P., Honoré, N., Seemann, T., Seeman, T., Stinear, T.P., and Brosch, R. (2014). A glimpse into the past and predictions for the future: the molecular evolution of the tuberculosis agent. Mol. Microbiol. *93*, 835–852.
Bottai, D., di Luca, M., Majlessi, L., Frigui, W., Simeone, R., Sayes, F., Bitter, W., Brennan, M.J., Leclerc, C., Batoni, G., et al. (2012). Disruption of the ESX-5 system of Mycobacterium tuberculosis causes loss of PPE protein secretion, reduction of cell wall integrity and strong attenuation. Mol. Microbiol. *83*, 1195–1209.
Bottai, D., Gröschel, M.I., and Brosch, R. (2017). Type VII Secretion Systems in Gram-Positive Bacteria. Curr. Top. Microbiol. Immunol. *404*, 235–265.
Bretl, D.J., Bigley, T.M., Terhune, S.S., and Zahrt, T.C. (2014). The MprB extracytoplasmic domain negatively regulates activation of the mycobacterium tuberculosis MprAB two-component system. J. Bacteriol. *196*, 391–406.
Brilha, S., Sathyamoorthy, T., Stuttaford, L.H., Walker, N.F., Wilkinson, R.J., Singh, S., Moores, R.C., Elkington, P.T., and Friedland, J.S. (2017). Early Secretory Antigenic Target-6 Drives Matrix Metalloproteinase-10 Gene Expression and Secretion in Tuberculosis. Am. J. Respir. Cell Mol. Biol. *56*, 223–232.
Brodin, P., Rosenkrands, I., Andersen, P., Cole, S.T., and Brosch, R. (2004). ESAT-6 proteins: protective antigens and virulence factors? Trends Microbiol. *12*, 500–508.
Brodin, P., de Jonge, M.I., Majlessi, L., Leclerc, C., Nilges, M., Cole, S.T., and Brosch, R. (2005). Functional analysis of early secreted antigenic target-6, the dominant T-cell antigen of Mycobacterium tuberculosis, reveals key residues involved in secretion, complex formation, virulence, and immunogenicity. J. Biol. Chem. *280*, 33953–33959.
Brodin, P., Majlessi, L., Marsollier, L., de Jonge, M.I., Bottai, D., Demangel, C., Hinds, J., Neyrolles, O., Butcher, P.D., Leclerc, C., et al. (2006). Dissection of ESAT-6 System 1 of Mycobacterium tuberculosis and Impact on Immunogenicity and Virulence. Infect. Immun. *74*, 88–98.
Calmette, A. (1931). Preventive Vaccination Against Tuberculosis with BCG. Proc. R. Soc. Med. *24*, 1481–1490.
Cambier, C.J., Falkow, S., and Ramakrishnan, L. (2014). Host Evasion and Exploitation Schemes of Mycobacterium tuberculosis. Cell *159*, 1497–1509.
Cambier, C.J., O'Leary, S.M., O'Sullivan, M.P., Keane, J., and Ramakrishnan, L. (2017). Phenolic Glycolipid Facilitates Mycobacterial Escape from Microbicidal Tissue-Resident Macrophages. Immunity *47*, 552–565.e4.
Cameron, T.A., and Zambryski, P.C. (2012). Disarming bacterial type IV secretion. Chem. Biol. *19*, 934–936.
Centers for Disease Control and Prevention (CDC) (2017). Reported Tuberculosis in the United States, 2016 (Atlanta, GA).
Champion, M.M., Williams, E.A., Pinapati, R.S., and Champion, P.A.D. (2014). Correlation of Phenotypic Profiles Using Targeted Proteomics Identifies Mycobacterial Esx-1 Substrates. J. Proteome Res. *13*, 5151–5164.
Chatterjee, S., Dwivedi, V.P., Singh, Y., Siddiqui, I., Sharma, P., Van Kaer, L., Chattopadhyay, D., and Das, G. (2011). Early secreted antigen ESAT-6 of Mycobacterium tuberculosis promotes

protective T helper 17 cell responses in a toll-like receptor-2-dependent manner. PLoS Pathog. *7*, e1002378.
Le Chevalier, F., Cascioferro, A., Frigui, W., Pawlik, A., Boritsch, E.C., Bottai, D., Majlessi, L., Herrmann, J.L., and Brosch, R. (2015). Revisiting the role of phospholipases C in virulence and the lifecycle of Mycobacterium tuberculosis. Sci. Rep. *5*, 16918.
Clerc, P., Baudry, B., and Sansonetti, P.J. (1986). Plasmid-mediated contact haemolytic activity in Shigella species: correlation with penetration into HeLa cells. Ann. Inst. Pasteur. Microbiol. *137A*, 267–278.
Comas, I., Coscolla, M., Luo, T., Borrell, S., Holt, K.E., Kato-Maeda, M., Parkhill, J., Malla, B., Berg, S., Thwaites, G., et al. (2013). Out-of-Africa migration and Neolithic coexpansion of Mycobacterium tuberculosis with modern humans. Nat. Genet. *45*, 1176–1182.
Conrad, W.H., Osman, M.M., Shanahan, J.K., Chu, F., Takaki, K.K., Cameron, J., Hopkinson-Woolley, D., Brosch, R., and Ramakrishnan, L. (2017). Mycobacterial ESX-1 secretion system mediates host cell lysis through bacterium contact-dependent gross membrane disruptions. Proc. Natl. Acad. Sci. U. S. A. *114*, 1371–1376.
Coros, A., Callahan, B., Battaglioli, E., and Derbyshire, K.M. (2008). The specialized secretory apparatus ESX-1 is essential for DNA transfer in Mycobacterium smegmatis. Mol. Microbiol. *69*, 794–808.
Cosma, C.L.C.L., Klein, K., Kim, R., Beery, D., and Ramakrishnan, L. (2006). Mycobacterium marinum Erp is a virulence determinant required for cell wall integrity and intracellular survival. Infect. Immun. *74*, 3125.
Cox, J., Hein, M.Y., Luber, C.A., Paron, I., Nagaraj, N., and Mann, M. (2014). Accurate Proteome-wide Label-free Quantification by Delayed Normalization and Maximal Peptide Ratio Extraction, Termed MaxLFQ. Mol. Cell. Proteomics *13*, 2513–2526.
Daniel, T.M. (2015). Jean-Antoine Villemin and the infectious nature of tuberculosis. Int. J. Tuberc. Lung Dis. *19*, 267–268.
Derrick, S.C., and Morris, S.L. (2007). The ESAT6 protein of Mycobacterium tuberculosis induces apoptosis of macrophages by activating caspase expression. Cell. Microbiol. *9*, 1547–1555.
Dey, B., Dey, R.J., Cheung, L.S., Pokkali, S., Guo, H., Lee, J.-H., and Bishai, W.R. (2015). A bacterial cyclic dinucleotide activates the cytosolic surveillance pathway and mediates innate resistance to tuberculosis. Nat. Med. *21*, 401–406.
Duncan, M.C., Linington, R.G., and Auerbuch, V. (2012). Chemical inhibitors of the type three secretion system: Disarming bacterial pathogens. Antimicrob. Agents Chemother. *56*, 5433–5441.
Elhay, M.J., Oettinger, T., and Andersen, P. (1998). Delayed-type hypersensitivity responses to ESAT-6 and MPT64 from Mycobacterium tuberculosis in the guinea pig. Infect. Immun. *66*, 3454–3456.
Elkington, P.T., Green, J.A., Emerson, J.E., Lopez-Pascua, L.D., Boyle, J.J., O'Kane, C.M., and Friedland, J.S. (2007). Synergistic up-regulation of epithelial cell matrix metalloproteinase-9 secretion in tuberculosis. Am. J. Respir. Cell Mol. Biol. *37*, 431–437.
Favrot, L., Grzegorzewicz, A.E., Lajiness, D.H., Marvin, R.K., Boucau, J., Isailovic, D., Jackson, M., and Ronning, D.R. (2013). Mechanism of inhibition of Mycobacterium tuberculosis antigen 85 by ebselen. Nat. Commun. *4*, 1–10.
Favrot, L., Lajiness, D.H., and Ronning, D.R. (2014). Inactivation of the Mycobacterium tuberculosis antigen 85 complex by covalent, allosteric inhibitors. J. Biol. Chem. *289*, 25031–

25040.
Fernandes da Costa, S.P., Savva, C.G., Bokori-Brown, M., Naylor, C.E., Moss, D.S., Basak, A.K., and Titball, R.W. (2014). Identification of a key residue for oligomerisation and pore-formation of Clostridium perfringens NetB. Toxins (Basel). *6*, 1049–1061.
Fortune, S.M., Jaeger, A., Sarracino, D.A., Chase, M.R., Sassetti, C.M., Sherman, D.R., Bloom, B.R., and Rubin, E.J. (2005). Mutually dependent secretion of proteins required for mycobacterial virulence. Proc. Natl. Acad. Sci. U. S. A. *102*, 10676–10681.
Francis, R.J., Butler, R.E., and Stewart, G.R. (2014). Mycobacterium tuberculosis ESAT-6 is a leukocidin causing Ca2+ influx, necrosis and neutrophil extracellular trap formation. Cell Death Dis. *5*, e1474.
Freer, J.H., Arbuthnott, J.P., and Bernheimer, A.W. (1968). Interaction of staphylococcal alpha-toxin with artificial and natural membranes. J. Bacteriol. *95*, 1153–1168.
Frigui, W., Bottai, D., Majlessi, L., Monot, M., Josselin, E., Brodin, P., Garnier, T., Gicquel, B., Martin, C., Leclerc, C., et al. (2008). Control of M. tuberculosis ESAT-6 secretion and specific T cell recognition by PhoP. PLoS Pathog. *4*, e33.
Ganguly, N., Giang, P.H., Gupta, C., Basu, S.K., Siddiqui, I., Salunke, D.M., and Sharma, P. (2008). Mycobacterium tuberculosis secretory proteins CFP-10, ESAT-6 and the CFP10:ESAT6 complex inhibit lipopolysaccharide-induced NF-kappaB transactivation by downregulation of reactive oxidative species (ROS) production. Immunol. Cell Biol. *86*, 98–106.
Gao, L.-Y., Guo, S., McLaughlin, B., Morisaki, H., Engel, J.N., and Brown, E.J. (2004). A mycobacterial virulence gene cluster extending RD1 is required for cytolysis, bacterial spreading and ESAT-6 secretion. Mol. Microbiol. *53*, 1677–1693.
Garces, A., Atmakuri, K., Chase, M.R., Woodworth, J.S., Krastins, B., Rothchild, A.C., Ramsdell, T.L., Lopez, M.F., Behar, S.M., Sarracino, D.A., et al. (2010). EspA acts as a critical mediator of ESX1-dependent virulence in Mycobacterium tuberculosis by affecting bacterial cell wall integrity. PLoS Pathog. *6*, e1000957.
Ghigo, E., Capo, C., Tung, C.-H., Raoult, D., Gorvel, J.-P., and Mege, J.-L. (2002). Coxiella burnetii survival in THP-1 monocytes involves the impairment of phagosome maturation: IFN-gamma mediates its restoration and bacterial killing. J. Immunol. *169*, 4488–4495.
Gray, T.A., Clark, R.R., Boucher, N., Lapierre, P., Smith, C., and Derbyshire, K.M. (2016). Intercellular communication and conjugation are mediated by ESX secretion systems in mycobacteria. Science (80-.). *354*, 347–350.
Gröschel, M.I., Sayes, F., Simeone, R., Majlessi, L., and Brosch, R. (2016). ESX secretion systems: mycobacterial evolution to counter host immunity. Nat. Rev. Microbiol. *14*, 677–691.
Guinn, K.M., Hickey, M.J., Mathur, S.K., Zakel, K.L., Grotzke, J.E., Lewinsohn, D.M., Smith, S., and Sherman, D.R. (2004). Individual RD1-region genes are required for export of ESAT-6/CFP-10 and for virulence of Mycobacterium tuberculosis. Mol. Microbiol. *51*, 359–370.
Hemmati, M., Seghatoleslam, A., Rasti, M., Ebadat, S., Naghibalhossaini, F., and Mostafavi-Pour, Z. (2016). Additive effect of recombinant Mycobacterium tuberculosis ESAT-6 protein and ESAT-6/CFP-10 fusion protein in adhesion of macrophages through fibronectin receptors. J. Microbiol. Immunol. Infect. *49*, 249–256.
Hertle, R., Brutsche, S., Groeger, W., Hobbie, S., Koch, W., Könninger, U., and Braun, V. (1997). Specific phosphatidylethanolamine dependence of Serratia marcescens cytotoxin activity. Mol. Microbiol. *26*, 853–865.
Hoiczyk, E., and Blobel, G. (2001). Polymerization of a single protein of the pathogen Yersinia enterocolitica into needles punctures eukaryotic cells. Proc. Natl. Acad. Sci. U. S. A. *98*, 4669–

4674.
Holmberg, S.D. (1990). The rise of tuberculosis in America before 1820. Am. Rev. Respir. Dis. *142*, 1228–1232.
Houben, D., Demangel, C., van Ingen, J., Perez, J., Baldeón, L., Abdallah, A.M., Caleechurn, L., Bottai, D., van Zon, M., de Punder, K., et al. (2012a). ESX-1-mediated translocation to the cytosol controls virulence of mycobacteria. Cell. Microbiol. *14*, 1287–1298.
Houben, E.N.G., Bestebroer, J., Ummels, R., Wilson, L., Piersma, S.R., Jiménez, C.R., Ottenhoff, T.H.M., Luirink, J., and Bitter, W. (2012b). Composition of the type VII secretion system membrane complex. Mol. Microbiol. *86*, 472–484.
Hsu, T., Hingley-Wilson, S.M., Chen, B., Chen, M., Dai, A.Z., Morin, P.M., Marks, C.B., Padiyar, J., Goulding, C., Gingery, M., et al. (2003). The primary mechanism of attenuation of bacillus Calmette-Guerin is a loss of secreted lytic function required for invasion of lung interstitial tissue. Proc. Natl. Acad. Sci. U. S. A. *100*, 12420–12425.
Izoré, T., Job, V., and Dessen, A. (2011). Biogenesis, regulation, and targeting of the type III secretion system. Structure *19*, 603–612.
Jamwal, S. V., Mehrotra, P., Singh, A., Siddiqui, Z., Basu, A., and Rao, K.V.S.S. (2016). Mycobacterial escape from macrophage phagosomes to the cytoplasm represents an alternate adaptation mechanism. Sci. Rep. *6*, 23089.
Johnson, B.K., Colvin, C.J., Needle, D.B., Mba Medie, F., Champion, P.A.D.D., and Abramovitch, R.B. (2015). The Carbonic Anhydrase Inhibitor Ethoxzolamide Inhibits the Mycobacterium tuberculosis PhoPR Regulon and Esx-1 Secretion and Attenuates Virulence. Antimicrob. Agents Chemother. *59*, 4436–4445.
de Jonge, M.I., Pehau-Arnaudet, G., Fretz, M.M., Romain, F., Bottai, D., Brodin, P., Honoré, N., Marchal, G., Jiskoot, W., England, P., et al. (2007). ESAT-6 from Mycobacterium tuberculosis dissociates from its putative chaperone CFP-10 under acidic conditions and exhibits membrane-lysing activity. J. Bacteriol. *189*, 6028–6034.
Joshi, S.A., Ball, D.A., Sun, M.G., Carlsson, F., Watkins, B.Y., Aggarwal, N., McCracken, J.M., Huynh, K.K., and Brown, E.J. (2012). EccA1, a component of the Mycobacterium marinum ESX-1 protein virulence factor secretion pathway, regulates mycolic acid lipid synthesis. Chem. Biol. *19*, 372–380.
Keller, C., Mellouk, N., Danckaert, A., Simeone, R., Brosch, R., Enninga, J., and Bobard, A. (2013). Single cell measurements of vacuolar rupture caused by intracellular pathogens. J. Vis. Exp. e50116.
Kennedy, G.M., Hooley, G.C., Champion, M.M., Mba Medie, F., and Champion, P.A.D. (2014). A novel ESX-1 locus reveals that surface-associated ESX-1 substrates mediate virulence in Mycobacterium marinum. J. Bacteriol. *196*, 1877–1888.
Kil, J., Lobarinas, E., Spankovich, C., Griffiths, S.K., Antonelli, P.J., Lynch, E.D., and Le Prell, C.G. (2017). Safety and efficacy of ebselen for the prevention of noise-induced hearing loss: A randomised, double-blind, placebo-controlled, phase 2 trial. Lancet *390*, 969–979.
King, C.H., Mundayoor, S., Crawford, J.T., and Shinnick, T.M. (1993). Expression of contact-dependent cytolytic activity by Mycobacterium tuberculosis and isolation of the genomic locus that encodes the activity. Infect. Immun. *61*, 2708–2712.
Kinhikar, A.G., Verma, I., Chandra, D., Singh, K.K., Weldingh, K., Andersen, P., Hsu, T., Jacobs, W.R., and Laal, S. (2010). Potential role for ESAT6 in dissemination of M. tuberculosis via human lung epithelial cells. Mol. Microbiol. *75*, 92–106.
Law, S., Piatek, A.S., Vincent, C., Oxlade, O., and Menzies, D. (2017). Emergence of drug

resistance in patients with tuberculosis cared for by the Indian health-care system: a dynamic modelling study. Lancet Public Heal. *2*, e47–e55.
Lawrence, S.L., Feil, S.C., Morton, C.J., Farrand, A.J., Mulhern, T.D., Gorman, M.A., Wade, K.R., Tweten, R.K., and Parker, M.W. (2015). Crystal structure of Streptococcus pneumoniae pneumolysin provides key insights into early steps of pore formation. Sci. Rep. *5*, 14352.
De Leon, J., Jiang, G., Ma, Y., Rubin, E., Fortune, S., and Sun, J. (2012). Mycobacterium tuberculosis ESAT-6 exhibits a unique membrane-interacting activity that is not found in its ortholog from non-pathogenic Mycobacterium smegmatis. J. Biol. Chem. *287*, 44184–44191.
van Leth, F., van der Werf, M.J., and Borgdorff, M.W. (2008). Prevalence of tuberculous infection and incidence of tuberculosis: a re-assessment of the Styblo rule. Bull. World Health Organ. *86*, 20–26.
Levitte, S., Adams, K.N., Berg, R.D., Cosma, C.L., Urdahl, K.B., and Ramakrishnan, L. (2016). Mycobacterial Acid Tolerance Enables Phagolysosomal Survival and Establishment of Tuberculous Infection In Vivo. Cell Host Microbe *20*, 250–258.
Lewis, K.N., Liao, R., Guinn, K.M., Hickey, M.J., Smith, S., Behr, M.A., and Sherman, D.R. (2003). Deletion of RD1 from Mycobacterium tuberculosis Mimics Bacille Calmette-Guérin Attenuation. J. Infect. Dis. *187*, 117–123.
Lin, K., O'Brien, K.M., Trujillo, C., Wang, R., Wallach, J.B., Schnappinger, D., and Ehrt, S. (2016). Mycobacterium tuberculosis Thioredoxin Reductase Is Essential for Thiol Redox Homeostasis but Plays a Minor Role in Antioxidant Defense. PLoS Pathog. *12*, e1005675.
Lou, Y., Rybniker, J., Sala, C., and Cole, S.T. (2017). EspC forms a filamentous structure in the cell envelope of Mycobacterium tuberculosis and impacts ESX-1 secretion. Mol. Microbiol. *103*, 26–38.
Lu, J., Vlamis-Gardikas, A., Kandasamy, K., Zhao, R., Gustafsson, T.N., Engstrand, L., Hoffner, S., Engman, L., and Holmgren, A. (2013). Inhibition of bacterial thioredoxin reductase: an antibiotic mechanism targeting bacteria lacking glutathione. FASEB J. *27*, 1394–1403.
Di Luca, M., Bottai, D., Batoni, G., Orgeur, M., Aulicino, A., Counoupas, C., Campa, M., Brosch, R., and Esin, S. (2012). The ESX-5 Associated eccB5-eccC5 Locus Is Essential for Mycobacterium tuberculosis Viability. PLoS One *7*.
Ma, Y., Keil, V., and Sun, J. (2015). Characterization of Mycobacterium tuberculosis EsxA membrane insertion: roles of N- and C-terminal flexible arms and central helix-turn-helix motif. J. Biol. Chem. *290*, 7314–7322.
Macdonald, S.H.-F., Woodward, E., Coleman, M.M., Dorris, E.R., Nadarajan, P., Chew, W.-M., McLaughlin, A.-M., and Keane, J. (2012). Networked T cell death following macrophage infection by Mycobacterium tuberculosis. PLoS One *7*, e38488.
MacGurn, J.A., and Cox, J.S. (2007). A Genetic Screen for Mycobacterium tuberculosis Mutants Defective for Phagosome Maturation Arrest Identifies Components of the ESX-1 Secretion System. Infect. Immun. *75*, 2668–2678.
Mahairas, G.G., Sabo, P.J., Hickey, M.J., Singh, D.C., and Stover, C.K. (1996). Molecular analysis of genetic differences between Mycobacterium bovis BCG and virulent M. bovis. J. Bacteriol. *178*, 1274–1282.
Mauch, V., Bonsu, F., Gyapong, M., Awini, E., Suarez, P., Marcelino, B., Melgen, R.E., Lönnroth, K., Nhung, N. V, Hoa, N.B., et al. (2013). Free tuberculosis diagnosis and treatment are not enough: patient cost evidence from three continents. Int. J. Tuberc. Lung Dis. *17*, 381–387.
McLaughlin, B., Chon, J.S., MacGurn, J.A., Carlsson, F., Cheng, T.L., Cox, J.S., and Brown,

E.J. (2007). A mycobacterium ESX-1-secreted virulence factor with unique requirements for export. PLoS Pathog. *3*, e105.
Mehra, A., Zahra, A., Thompson, V., Sirisaengtaksin, N., Wells, A., Porto, M., Köster, S., Penberthy, K., Kubota, Y., Dricot, A., et al. (2013). Mycobacterium tuberculosis type VII secreted effector EsxH targets host ESCRT to impair trafficking. PLoS Pathog. *9*, e1003734.
Miles, A.A., Misra, S.S., and Irwin, J.O. (1938). The estimation of the bactericidal power of the blood. J. Hyg. (Lond). *38*, 732–749.
Mostowy, S., Cleto, C., Sherman, D.R., and Behr, M.A. (2004). The Mycobacterium tuberculosis complex transcriptome of attenuation. Tuberculosis (Edinb). *84*, 197–204.
Newton-Foot, M., Warren, R.M., Sampson, S.L., Van Helden, P.D., and Gey Van Pittius, N.C. (2016). The plasmid-mediated evolution of the mycobacterial ESX (Type VII) secretion systems. BMC Evol. Biol. *16*, 1–12.
Niederweis, M., Danilchanka, O., Huff, J., Hoffmann, C., and Engelhardt, H. (2010). Mycobacterial outer membranes: in search of proteins. Trends Microbiol. *18*, 109–116.
Okkels, L.M., and Andersen, P. (2004). Protein-protein interactions of proteins from the ESAT-6 family of Mycobacterium tuberculosis. J. Bacteriol. *186*, 2487–2491.
Pang, X., Samten, B., Cao, G., Wang, X., Tvinnereim, A.R., Chen, X.L., and Howard, S.T. (2013). MprAB regulates the espA operon in Mycobacterium tuberculosis and modulates ESX-1 function and host cytokine response. J. Bacteriol. *195*, 66–75.
Peng, X., and Sun, J. (2016). Mechanism of ESAT-6 membrane interaction and its roles in pathogenesis of Mycobacterium tuberculosis. Toxicon *116*, 29–34.
Peng, X., Jiang, G., Liu, W., Zhang, Q., Qian, W., and Sun, J. (2016). Characterization of differential pore-forming activities of ESAT-6 proteins from Mycobacterium tuberculosis and Mycobacterium smegmatis. FEBS Lett. *590*, 509–519.
Peñuelas-Urquides, K., Villarreal-Treviño, L., Silva-Ramírez, B., Rivadeneyra-Espinoza, L., Said-Fernández, S., de León, M.B., and León, M.B. de (2013). Measuring of Mycobacterium tuberculosis growth. A correlation of the optical measurements with colony forming units. Braz. J. Microbiol. *44*, 287–289.
Portal-Celhay, C., Tufariello, J.M., Srivastava, S., Zahra, A., Klevorn, T., Grace, P.S., Mehra, A., Park, H.S., Ernst, J.D., Jacobs, W.R., et al. (2016). Mycobacterium tuberculosis EsxH inhibits ESCRT-dependent CD4+T-cell activation. Nat. Microbiol. *2*, 1–9.
Price, N.M., Farrar, J., Tran, T.T., Nguyen, T.H., Tran, T.H., and Friedland, J.S. (2001). Identification of a matrix-degrading phenotype in human tuberculosis in vitro and in vivo. J. Immunol. *166*, 4223–4230.
Pym, A.S., Brodin, P., Brosch, R., Huerre, M., and Cole, S.T. (2002). Loss of RD1 contributed to the attenuation of the live tuberculosis vaccines Mycobacterium bovis BCG and Mycobacterium microti. Mol. Microbiol. *46*, 709–717.
Pym, A.S., Brodin, P., Majlessi, L., Brosch, R., Demangel, C., Williams, A., Griffiths, K.E., Marchal, G., Leclerc, C., and Cole, S.T. (2003). Recombinant BCG exporting ESAT-6 confers enhanced protection against tuberculosis. Nat. Med. *9*, 533–539.
Quigley, J., Hughitt, V.K., Velikovsky, C.A., Mariuzza, R.A., El-Sayed, N.M., and Briken, V. (2017). The Cell Wall Lipid PDIM Contributes to Phagosomal Escape and Host Cell Exit of Mycobacterium tuberculosis. MBio *8*, e00148-17.
Ragle, B.E., and Bubeck Wardenburg, J. (2009). Anti-alpha-hemolysin monoclonal antibodies mediate protection against Staphylococcus aureus pneumonia. Infect. Immun. *77*, 2712–2718.
Ramakrishnan, L., and Falkow, S. (1994). Mycobacterium marinum persists in cultured

mammalian cells in a temperature-restricted fashion. Infect. Immun. *62*, 3222–3229.
Ramsdell, T.L., Huppert, L.A., Sysoeva, T.A., Fortune, S.M., and Burton, B.M. (2015). Linked Domain Architectures Allow for Specialization of Function in the FtsK/SpoIIIE ATPases of ESX Secretion Systems. J. Mol. Biol. *427*, 1119–1132.
Ravn, P., Demissie, A., Eguale, T., Wondwosson, H., Lein, D., Amoudy, H.A., Mustafa, A.S., Jensen, A.K., Holm, A., Rosenkrands, I., et al. (1999). Human T cell responses to the ESAT-6 antigen from Mycobacterium tuberculosis. J. Infect. Dis. *179*, 637–645.
Ray, K., Marteyn, B., Sansonetti, P.J., and Tang, C.M. (2009). Life on the inside: the intracellular lifestyle of cytosolic bacteria. Nat. Rev. Microbiol. *7*, 333–340.
Refai, A., Haoues, M., Othman, H., Barbouche, M.R., Moua, P., Bondon, A., Mouret, L., Srairi-Abid, N., and Essafi, M. (2015). Two distinct conformational states of Mycobacterium tuberculosis virulent factor early secreted antigenic target 6 kDa are behind the discrepancy around its biological functions. FEBS J. *282*, 4114–4129.
Renshaw, P.S., Lightbody, K.L., Veverka, V., Muskett, F.W., Kelly, G., Frenkiel, T.A., Gordon, S. V, Hewinson, R.G., Burke, B., Norman, J., et al. (2005). Structure and function of the complex formed by the tuberculosis virulence factors CFP-10 and ESAT-6. EMBO J. *24*, 2491–2498.
van Rooijen, N., and Hendrikx, E. (2010). Liposomes for specific depletion of macrophages from organs and tissues. In Methods in Molecular Biology (Clifton, N.J.), pp. 189–203.
Rosenberg, O.S.S., Dovala, D., Li, X., Connolly, L., Bendebury, A., Finer-Moore, J., Holton, J., Cheng, Y., Stroud, R.M.M., and Cox, J.S.S. (2015). Substrates Control Multimerization and Activation of the Multi-Domain ATPase Motor of Type VII Secretion. Cell 1–12.
Rybniker, J., Chen, J.M., Sala, C., Hartkoorn, R.C., Vocat, A., Benjak, A., Boy-Röttger, S., Zhang, M., Székely, R., Greff, Z., et al. (2014). Anticytolytic Screen Identifies Inhibitors of Mycobacterial Virulence Protein Secretion. Cell Host Microbe *16*, 538–548.
Sani, M., Houben, E.N.G., Geurtsen, J., Pierson, J., de Punder, K., van Zon, M., Wever, B., Piersma, S.R., Jiménez, C.R., Daffé, M., et al. (2010). Direct visualization by cryo-EM of the mycobacterial capsular layer: a labile structure containing ESX-1-secreted proteins. PLoS Pathog. *6*, e1000794.
Sassetti, C.M., and Rubin, E.J. (2003). Genetic requirements for mycobacterial survival during infection. Proc. Natl. Acad. Sci. U. S. A. *100*, 12989–12994.
Shaw, R.K., Daniell, S., Ebel, F., Frankel, G., and Knutton, S. (2001). EspA filament-mediated protein translocation into red blood cells. Cell. Microbiol. *3*, 213–222.
Simeone, R., Bobard, A., Lippmann, J., Bitter, W., Majlessi, L., Brosch, R., and Enninga, J. (2012). Phagosomal rupture by Mycobacterium tuberculosis results in toxicity and host cell death. PLoS Pathog. *8*, e1002507``.
Singh, N., Halliday, A.C., Thomas, J.M., Kuznetsova, O. V, Baldwin, R., Woon, E.C.Y.Y., Aley, P.K., Antoniadou, I., Sharp, T., Vasudevan, S.R., et al. (2013). A safe lithium mimetic for bipolar disorder. Nat. Commun. *4*, 1332–1337.
Smith, J., Manoranjan, J., Pan, M., Bohsali, A., Xu, J., Liu, J., McDonald, K.L., Szyk, A., LaRonde-LeBlanc, N., and Gao, L.-Y. (2008). Evidence for Pore Formation in Host Cell Membranes by ESX-1-Secreted ESAT-6 and Its Role in Mycobacterium marinum Escape from the Vacuole. Infect. Immun. *76*, 5478–5487.
Solomonson, M., Setiaputra, D., Makepeace, K.A.T.A.T., Lameignere, E., Petrotchenko, E.V. V., Conrady, D.G.G., Bergeron, J.R.R., Vuckovic, M., DiMaio, F., Borchers, C.H.H., et al. (2015). Structure of EspB from the ESX-1 type VII secretion system and insights into its export

mechanism. Structure *23*, 571–583.
Speer, A., Sun, J., Danilchanka, O., Meikle, V., Rowland, J.L., Walter, K., Buck, B.R., Pavlenok, M., Hölscher, C., Ehrt, S., et al. (2015). Surface hydrolysis of sphingomyelin by the outer membrane protein Rv0888 supports replication of Mycobacterium tuberculosis in macrophages. Mol. Microbiol. *97*, 881–897.
Stanley, S. a, Raghavan, S., Hwang, W.W., and Cox, J.S. (2003). Acute infection and macrophage subversion by Mycobacterium tuberculosis require a specialized secretion system. Proc. Natl. Acad. Sci. *100*, 13001–13006.
Swaim, L.E., Connolly, L.E., Volkman, H.E., Humbert, O., Born, D.E., and Ramakrishnan, L. (2006). Mycobacterium marinum infection of adult zebrafish causes caseating granulomatous tuberculosis and is moderated by adaptive immunity. Infect. Immun. *74*, 6108–6117.
Takaki, K., Cosma, C.L., Troll, M.A., and Ramakrishnan, L. (2012). An in vivo platform for rapid high-throughput antitubercular drug discovery. Cell Rep. *2*, 175–184.
Takaki, K., Davis, J.M., Winglee, K., and Ramakrishnan, L. (2013). Evaluation of the pathogenesis and treatment of Mycobacterium marinum infection in zebrafish. Nat. Protoc. *8*, 1114–1124.
Tameris, M.D., Hatherill, M., Landry, B.S., Scriba, T.J., Snowden, M.A., Lockhart, S., Shea, J.E., McClain, J.B., Hussey, G.D., Hanekom, W.A., et al. (2013). Safety and efficacy of MVA85A, a new tuberculosis vaccine, in infants previously vaccinated with BCG: a randomised, placebo-controlled phase 2b trial. Lancet (London, England) *381*, 1021–1028.
Tekaia, F., Gordon, S. V, Garnier, T., Brosch, R., Barrell, B.G., and Cole, S.T. (1999). Analysis of the proteome of Mycobacterium tuberculosis in silico. Tuber. Lung Dis. *79*, 329–342.
Thangamani, S., Younis, W., and Seleem, M.N. (2015). Repurposing Clinical Molecule Ebselen to Combat Drug Resistant Pathogens. PLoS One *10*, e0133877.
Tiemersma, E.W., van der Werf, M.J., Borgdorff, M.W., Williams, B.G., and Nagelkerke, N.J.D. (2011). Natural history of tuberculosis: duration and fatality of untreated pulmonary tuberculosis in HIV negative patients: a systematic review. PLoS One *6*, e17601.
Tufariello, J.M., Chapman, J.R., Kerantzas, C.A., Wong, K.-W., Vilchèze, C., Jones, C.M., Cole, L.E., Tinaztepe, E., Thompson, V., Fenyö, D., et al. (2016). Separable roles for Mycobacterium tuberculosis ESX-3 effectors in iron acquisition and virulence. Proc. Natl. Acad. Sci. U. S. A. *113*, E348-57.
Tyanova, S., Temu, T., Sinitcyn, P., Carlson, A., Hein, M.Y., Geiger, T., Mann, M., and Cox, J. (2016). The Perseus computational platform for comprehensive analysis of (prote)omics data. Nat. Methods *13*, 731–740.
Vandenesch, F., Lina, G., and Henry, T. (2012). Staphylococcus aureus hemolysins, bi-component leukocidins, and cytolytic peptides: a redundant arsenal of membrane-damaging virulence factors? Front. Cell. Infect. Microbiol. *2*, 12.
Veneman, W.J., Marín-Juez, R., de Sonneville, J., Ordas, A., Jong-Raadsen, S., Meijer, A.H., and Spaink, H.P. (2014). Establishment and optimization of a high throughput setup to study Staphylococcus epidermidis and Mycobacterium marinum infection as a model for drug discovery. J. Vis. Exp. e51649.
Veyrier, F., Pletzer, D., Turenne, C., and Behr, M.A. (2009). Phylogenetic detection of horizontal gene transfer during the step-wise genesis of Mycobacterium tuberculosis. BMC Evol. Biol. *9*, 1–14.
Volkman, H.E., Clay, H., Beery, D., Chang, J.C.W., Sherman, D.R., and Ramakrishnan, L. (2004). Tuberculous granuloma formation is enhanced by a mycobacterium virulence

determinant. PLoS Biol. *2*, e367.
Volkman, H.E., Pozos, T.C., Zheng, J., Davis, J.M., Rawls, J.F., and Ramakrishnan, L. (2010). Tuberculous Granuloma Induction via Interaction of a Bacterial Secreted Protein with Host Epithelium. Science (80-.). *327*, 466–469.
Walker, D.H., Feng, H.M., and Popov, V.L. (2001). Rickettsial phospholipase A2 as a pathogenic mechanism in a model of cell injury by typhus and spotted fever group rickettsiae. Am. J. Trop. Med. Hyg. *65*, 936–942.
Walker, G., Hertle, R., and Braun, V. (2004). Activation of Serratia marcescens hemolysin through a conformational change. Infect. Immun. *72*, 611–614.
Wang, X., Barnes, P.F., Dobos-Elder, K.M., Townsend, J.C., Chung, Y., Shams, H., Weis, S.E., and Samten, B. (2009). ESAT-6 inhibits production of IFN-gamma by Mycobacterium tuberculosis-responsive human T cells. J. Immunol. *182*, 3668–3677.
Wards, B.J.J., de Lisle, G.W.W., and Collins, D.M.M. (2000). An esat6 knockout mutant of Mycobacterium bovis produced by homologous recombination will contribute to the development of a live tuberculosis vaccine. Tuber. Lung Dis. *80*, 185–189.
Wassermann, R., Gulen, M.F.F., Sala, C., Perin, S.G.G., Lou, Y., Rybniker, J., Schmid-Burgk, J.L.L., Schmidt, T., Hornung, V., Cole, S.T.T., et al. (2015). Mycobacterium tuberculosis Differentially Activates cGAS- and Inflammasome-Dependent Intracellular Immune Responses through ESX-1. Cell Host Microbe *17*, 799–810.
Watson, R.O., Manzanillo, P.S., and Cox, J.S. (2012). Extracellular M. tuberculosis DNA Targets Bacteria for Autophagy by Activating the Host DNA-Sensing Pathway. Cell *150*, 803–815.
van der Wel, N., Hava, D., Houben, D., Fluitsma, D., van Zon, M., Pierson, J., Brenner, M., and Peters, P.J. (2007). M. tuberculosis and M. leprae translocate from the phagolysosome to the cytosol in myeloid cells. Cell *129*, 1287–1298.
World Health Organization (2017). Global Tuberculosis Report 2017 (Geneva).
Yamaguchi, T., Sano, K., Takakura, K., Saito, I., Shinohara, Y., Asano, T., and Yasuhara, H. (1998). Ebselen in acute ischemic stroke: a placebo-controlled, double-blind clinical trial. Ebselen Study Group. Stroke *29*, 12–17.